Environmental Microbiology

ENVIRONMENTAL MICROBIOLOGY

RESEARCH ARTICLE OPEN ACCESS

Phylogenomics Untangles the Metabolic Potential of *Picochlorum tauri*, a New Picoalgal Species Causing a Winter Bloom in the Mediterranean Thau Lagoon

Béatrice Bec[1] | Franck Lagarde[2] | Angélique Gobet[2] | Riccardo Aiese Cigliano[3] | Marco Di Marsico[3] | Jean-Michel Hermel[4] | Marion Richard[2] | Emilie Le Floc'h[2] | Robert van Lis[5] | Ariane Atteia[2]

[1]MARBEC, Univ Montpellier, CNRS, Ifremer, IRD, Montpellier, France | [2]MARBEC, Univ Montpellier, CNRS, Ifremer, IRD, Sète, France | [3]Sequentia Biotech SL, Barcelona, Spain | [4]Observatoire Océanologique de Banyuls, Biopic, Banyuls-sur-Mer, France | [5]LBE, Univ Montpellier, INRAE, Narbonne, France

Correspondence: Ariane Atteia (ariane.atteia@cnrs.fr)

Received: 31 March 2025 | **Revised:** 25 August 2025 | **Accepted:** 29 August 2025

Funding: A.A. and E.L.F. acknowledge support from the Centre National de la Recherche Scientifique (CNRS), B.B. acknowledges support from the University of Montpellier and R.v.L. acknowledges support from the National Research Institute for Agriculture, Food and the Environment (INRAE). A.G., F.L. and M.R. received support from the Institut Français de Recherche pour l'Exploitation de la Mer (IFREMER). This work received financial support from the Ministère de l'Environnement, de l'Agriculture et de l'Alimentation (DPMA), Région Occitanie, Département de l'Hérault, Sète Agglopôle Méditerranée and Department of Oceanography and Ecosystem Dynamic of IFREMER (OVERTE; convention 19/2 217 111), from the Scientific Direction of IFREMER (PICOTHAU; ref. 1000730). This work has also received financial support from the CNRS through the MITI interdisciplinary (pHEATo; 238945), and the support of LabEx CeMEB, an ANR 'Investissements d'avenir' Program (ANR-10-LABX-04-01).

Keywords: carbon metabolism | marine algae | metabolic plasticity | photosynthetic picoeukaryote | propionyl-CoA | trebouxiophyceans | vitamin

ABSTRACT

In the winter of 2018–2019, the Mediterranean Thau lagoon experienced an intense green bloom with severe ecological consequences. Here, we aimed at identifying the blooming species and deciphering its metabolic potential. The blooming alga was identified by a metabarcoding approach and later isolated in an axenic form. High-quality nuclear and organellar genome sequences were generated. Phylogenetic and phylogenomic analyses revealed that the alga is a new member of the genus *Picochlorum* (Trebouxiophyceae, Chlorophyta) that we named *Picochlorum tauri*. Comparative genomic analyses were conducted to provide insights into (i) genome reduction in the *Picochlorum* genus with respect to other trebouxiophycean genera and (ii) the metabolic specificities of *P. tauri* with respect to other eukaryotic picophytoplankton. Genome mining unveiled in *P. tauri* an extended gene repertoire for carbon concentrating mechanisms, a reduced number of routes for acetyl-CoA synthesis from pyruvate and citrate, and a vitamin B12-dependent carboxylation pathway for propionyl-CoA breakdown. By contrast to the surveyed photosynthetic picoeukaryotes, *P. tauri* has specific functional traits linked to carbon metabolism, vitamin and chlorophyll synthesis, which are expected to boost physiology. These traits might have contributed to the fast development and maintenance of *P. tauri* in cool waters under low solar radiance.

1 | Introduction

The size and taxonomic structure of phytoplankton communities regulate the functioning of marine ecosystems and biogeochemical cycles in the global ocean (Legendre and Le Fèvre 1991; Hood et al. 2006). Phytoplankton blooms are considered the main event influencing ecosystem richness (D'Ortenzio and Ribera d'Alcalà 2008; Lazzari et al. 2012). They are observed in open ocean waters as well as in coastal waters and are formed naturally or as a consequence of anthropogenic activities

(Beman et al. 2005). In the northwestern Mediterranean Sea, the phytoplankton seasonal dynamics have been reported to follow a typical temperate cycle, with increased biomass in late winter/early spring and very low values in summer. In coastal regions, algal proliferations are sporadic and usually develop in response to changing environmental conditions, such as high nutrient inputs or strong salinity gradients (Paerl 2006; D'Ortenzio and Ribera d'Alcalà 2008; Mignot et al. 2016). Overall, the proliferation of algae reflects a degree of uncoupling between primary production and phytoplankton biomass loss, resulting from grazing by zooplankton, viral lysis and sedimentation to the seafloor (Legendre 1990; Townsend et al. 1994). Algal blooms are generally beneficial, fixing carbon at the base of the food chain and supporting ecosystems worldwide. However, they can lead to disease or mortality of marine species and humans through the production of a variety of toxins or depletion of oxygen in bottom waters, a consequence of the decay of a dense algal bloom (Anderson 1997; Brush et al. 2020).

Bloom dynamics, from the initiation to the collapse, are typically inferred from bulk measurements, satellite data and model outputs. Algal proliferations typically affect the colour of the water, and analyses of Chl*a* and other pigments maps allow reaching an understanding of bloom phenology (Arrigo et al. 1999; Negrete-García et al. 2024). A fine understanding of the algal species successions during a bloom can be inferred from microscopic observations and molecular techniques, including qPCR, metabarcoding or metagenome sequencing (Arrigo et al. 1999; Delmont et al. 2015; Cui et al. 2021). Molecular techniques are particularly useful for very small phytoplankton ($<3\,\mu m$ in diameter), also referred to as picophytoplankton, because distinctive morphological features are often absent. Picophytoplankton comprises a prokaryotic component, dominated by the cyanobacteria *Prochlorococcus* and *Synechococcus* in the ocean (Buitenhuis et al. 2012), and a eukaryotic component which is much more diverse. Photosynthetic picoeukaryotes (hereinafter PPE) in marine waters belong to various supergroups, including the Bacillariophyta (TSAR, Stramenopiles), Dinophyceae (TSAR, Alveolata), Haptophyceae (Haptista) and Chlorophyta (Archaeplastida) (Tragin and Vaulot 2018; Pierella Karlusich et al. 2020; Burki et al. 2020). High-throughput sequencing of short DNA barcode regions, also known as metabarcoding, allows characterising species assemblages in diverse environmental samples. This technique has, for example, shown that PPEs of the Mamiellophyceae class (Chlorophyta), specifically those of the genera *Ostreococcus*, *Micromonas* and *Bathycoccus*, were dominant in ocean spring phytoplankton blooms in the North Atlantic Subtropical Gyre (Bolaños et al. 2020; Eckmann et al. 2024).

The Thau lagoon, located on the French Mediterranean coast, is the largest basin in the Occitanie region. It is separated from the Mediterranean Sea by a sandbank 20 km long, has a surface area of 6790 ha and an average depth of 4.5 m (Fiandrino et al. 2017). About 20% of the lagoon's total surface area is exploited by shellfish farming (Hamon and Tournier 1984). The economic and scientific importance of the lagoon ecosystem has prompted extensive research on the seawater and phytoplankton composition (Troussellier and Deslous-Paoli 2001; Derolez, Soudant, et al. 2020; Derolez, Malet, et al. 2020). In addition, nutrient loadings have been measured fortnightly since 2017 (Lagarde et al. 2021; PHYTOBS 2024). The abundance of PPEs in this lagoon was revealed more than three decades ago through flow cytometry studies (Vaquer et al. 1996; Chrétiennot-Dinet and Courties 1997). The smallest known eukaryote, *Ostreococcus tauri* (Courties et Chrétiennot-Dinet), was isolated from the lagoon, and it was described as the dominant PPE, present throughout the year with low seasonal fluctuations (Courties et al. 1994; Chrétiennot-Dinet et al. 1995; Vaquer et al. 1996). In the winter of 2018–2019, the Mediterranean Thau lagoon experienced an intense green bloom with severe consequences on the local shellfish economies (Lagarde et al. 2021; Richard et al. 2022). As observed by the ECOSCOPA oyster observatory network (Lagarde et al. 2025), the bloom halted growth and caused weight loss in Pacific oysters (Richard et al. 2022), resulting in important mortalities in autumn 2018 and winter 2019 (Fleury et al. 2020). The bloom was unprecedented, with exceptional duration and high chlorophyll biomass, unseen since the early 2000s when the Water Framework Directive (WFD) was adopted and the coastal lagoon initiated an oligotrophication trajectory (Bec et al. 2011; Derolez, Soudant, et al. 2020). The overall aim of the directive was to combat water pollution, including eutrophication of European aquatic ecosystems, and achieve good ecological status. The implementation of the WFD in the Thau lagoon has led to a significant reduction in nutrient concentrations and phytoplankton biomass (Derolez, Soudant, et al. 2020). In the present study, we developed a multifaceted approach to identify the photosynthetic algal species responsible for the prolonged bloom and explore their metabolic potential. Our data showed that the dominant alga belonged to the genus *Picochlorum* (Trebouxiophyceae, Chlorophyta), thereby constituting the first report of a winter bloom for this genus. The genome data indicated that the bloom-forming alga represented a new strain, which we named *Picochlorum tauri* Hemon & Grimsley, sp. nov. Our comparative genomics approach unveiled metabolic traits linked to carbon metabolism, and vitamin and chlorophyll syntheses, which are believed to have contributed to the picoalgal ecological success in cool waters and low solar radiance.

2 | Methods

2.1 | Algal Isolation and Molecular Identification

The algal strain was isolated from surface water samples (1 m depth) collected on 01/10/2019 in the Thau Lagoon (France) at the site of Bouzigues (GPS WGS84: Long 3.66463°E, Lat 43.43429°N). Early January 2019, the lagoon waters were characterised by temperatures of 6.2°C–7.0°C, and salinities of 36.0–36.3; nitrogen loads were below the limit of quantification, and phosphate concentrations fluctuated between 0 and $0.15\,\mu mol\,L^{-1}$ (Lagarde et al. 2021; Table S1). Water samples were diluted once in Guillard's (f/2) Marine Water Enrichment Solution (Sigma-Aldrich) containing 3.5% (w/v) sea salts (Sigma-Aldrich) (f/2 medium) and maintained at 14°C, with a photoperiod of 12 h:12 h light:dark, and light intensity of $50\,\mu mol$ photons $m^{-2}s^{-1}$. Following algal growth, serial dilutions in f/2 medium supplemented with ampicillin at $100\,\mu g\,mL^{-1}$ to limit bacterial growth were carried out. Establishment of an axenic unialgal culture was achieved by treatments with antibiotics (ampicillin and cefotaxime) and streaking on agar plates.

The alga was later cultivated in a modified f/2 medium, hereafter called PiF medium, with a salt base adapted from Kester et al. (1967). The components and their final concentrations in the defined PiF medium (prepared in MilliQ water) were as follows: NaCl (420 mM), KCl (10 mM), $NaHCO_3$ (2 mM), H_3BO_3 (0.43 mM), $MgCl_2{\cdot}6H_2O$ (20 mM), $MgSO_4{\cdot}7H_2O$ (10 mM), $CaCl_2{\cdot}2H_2O$ (5 mM), Fe·EDTA (14.7 mM), $CuSO_4{\cdot}5H_2O$ (39 μM), $Na_2MoO_4{\cdot}2H_2O$ (260 μM), $ZnSO_4{\cdot}7H_2O$ (76.5 μM), $CoCl_2{\cdot}6H_2O$ (42 μM), $MnCl_2{\cdot}4H_2O$ (910 μM), $NaH_2PO_4{\cdot}H_2O$ (36 μM) and $NaNO_3$ (882 μM). The PiF medium has an average pH of 8.0 and a salinity of 29.5. Since its isolation as an axenic mono-strain (about 6 years ago), the alga was maintained on the vitamin-free PiF medium, either in liquid culture or on agar plates, at 20°C, under a 12 h:12 h light:dark cycle, at 50 μmol photons m^{-2} s^{-1}. The effect of exogenous vitamins on the algal growth was evaluated after addition in the PiF medium of thiamine hydrochloride (B1), biotin (B7) and cyanocobalamin (B12) at final concentrations of 5 μM, 0.1 μM and 0.1 μM, respectively. The cultures (100 mL) were carried out in triplicate in 250 mL Erlenmeyer flasks at 22°C, under a 14 h:10 h light:dark cycle (100 μmol photons m^{-2} s^{-1}), and shaking at 140 rpm. Algal growth was monitored using a Malassez cell counting chamber.

For molecular identification of the isolated strain, a 5-mL culture aliquot was sampled and centrifuged for 10 min at 5000 *g* at RT. Genomic DNA was extracted using a phenol/chloroform method (Lacroux et al. 2022), and the region covering the ribosomal DNA operon (18S rDNA-ITSs-first 500 bp of the 26S rDNA) was amplified using the primer set EAF3 and ITS055 as described in (Lacroux et al. 2022). Both amplicon strands were sequenced at Eurofins Genomics (Cologne, Germany), using universal and specific primers (Table S2).

2.2 | Chl*a* Survey and Flow Cytometry Analyses

Water samples were collected by the PHYTOBS monitoring network (Belin et al. 2021) bimonthly at the Bouzigues and Marseillan stations. Water samples (50 mL) were filtered under vacuum (< 10 cm Hg) on Whatman GF/F membranes (0.7-μm pore size). The filters were stored at −20°C until analysis. For pigment extraction, the filters were ground in 90% acetone and stored for 24 h in the dark at 4°C. Chl*a* concentrations were measured by monochromatic spectrophotometry (Aminot and Kérouel 2004).

The picophytoplankton abundances were determined with a FACSCalibur flow cytometer (Becton Dickinson) fitted with a 15-mW argon laser (488 excitation) as described in Bec et al. (2011). Water samples (1 mL) were fixed with 2% (final concentration) formaldehyde and stored in liquid nitrogen. Samples were analysed with a mixture of fluorescent beads ('Fluoresbrite' YG, Polysciences) of various nominal sizes (1, 2 and 3 μm) to identify the size range of phytoplankton. Photosynthetic picoeukaryotes (≤ 3 μm) were distinguished on the basis of red fluorescence (FL3, related to Chl*a* fluorescence; wavelength > 650 nm) and light diffraction (FSC, related to cell size). Phycoerythrin-rich picocyanobacteria (< 1 μm, PE-CYAN) were discriminated from other photosynthetic organisms by their strong orange fluorescence (FL2, related to phycoerythrin fluorescence; wavelength 542–585 nm) and light diffraction (Bec et al. 2011).

2.3 | Transmission Electron Microscopy (TEM)

For TEM, mid-exponential phase *P. tauri* cells were prepared according to Derelle et al. (2008). The cells were fixed with glutaraldehyde at a final concentration of 1% in their culture medium and then centrifuged for 15 min at 3000 *g*. The cell pellet was mixed rapidly with 40 μL of 1% low-melting agarose (Type II, Sigma) maintained at 37°C, and aspirated into the disposable glass tube of a positive displacement micropipette (SMI, Emerville, CA, USA). With the glass tube placed in ice, the agarose jellifies quickly; a 'noodle' containing the cells was extruded on an ice-cold watch glass and cut into 2- to 3-mm-long pieces. The noodles were fixed for 2 h at 4°C in 2.5% glutaraldehyde with one volume of 0.13 M cacodylate buffer pH 7.2–7.4 in culture medium, and then washed three times for 30 min in one volume 0.2 M cacodylate buffer in culture medium. Noodles were postfixed in 1% OsO_4 in 0.2 M cacodylate buffer at room temperature for 1 h, washed in 0.2 M cacodylate buffer, dehydrated in successive concentrations of ethyl alcohol (30%, 50%, 75%, 95% and 100%), then in propylene oxide. After embedding in Epon 812 resin, noodles were polymerised at 60°C for 2 days. Ultrathin sections of 70 nm cut on a Leica Ultracut R ultramicrotome were stained with uranyl acetate and lead citrate before examination on a H7500 Hitachi transmission electron microscope.

2.4 | Environmental Metabarcoding

Surface water samples (1 m depth) were collected in triplicate (150 mL) at the shellfish farming site of Bouzigues on the following dates: 6 December 2018, 7 January 2019, 11 February 2019 and 26 February 2019. Water samples were centrifuged at 3100 *g* for 30 min at 10°C, and the resulting pellets were immediately flash frozen and stored at −80°C. From each individual pellet, DNA was extracted using the phenol/chloroform method, as described in Atteia et al. (2024). Aliquots (20 μL) of the triplicates were pooled and further cleaned with OneStep PCR Inhibitor Removal (Ozyme). DNA quantification was carried out using the dsDNA BR Assay Kit on a Qubit fluorometer (ThermoFisher Scientific). Libraries and MiSeq sequencing were performed by LGC Biosearch Technologies (Berlin, Germany). Amplification of the V4 variable region of the 18S rRNA gene was carried out using eukaryotic-specific universal primers (TAReuk454FWD1: 5′-CCAGCASCYGCGGTAATTCC-3′ and TAReukREV3mo: 5′-ACTTTCGTTCTTGATYRATGA-3′) (Piredda et al. 2017; Stoeck et al. 2010). Amplicons were sequenced using a 2 × 300 bp paired-end V3 kit. Raw Illumina sequences were preprocessed through the LGC Biosearch Technologies pipeline: libraries were demultiplexed using the Illumina bcl2fastq 2.17.1.14 software (https://support.illumina.com/sequencing/sequencing_software/bcl2fastq-conversion-software.html); sequences without barcodes/primers or conflicting barcode/primer pairs were discarded; Illumina adapters, barcode and primer sequences were removed; sequences were then processed in R v4.2.2 (R Core Team 2021) using the dada2 package (Callahan et al. 2016) as described in Atteia et al. (2024), where default parameters were used for all functions but for filterAndTrim where maxEE = c(2,5) was chosen. This sequence processing allowed for removing low-quality sequences, merging overlapping paired-end sequences together, clustering sequences into

amplicon sequence variants (ASVs), removing PCR chimaeras and taxonomically assigning ASVs using the PR2 SSU database version 4.14.0 (https://pr2-database.org/) (Guillou et al. 2012).

2.5 | Phylogeny Inferred From 18S rDNA Sequences

Sequences of 18S rDNA from 26 Chlorophytes, including that of *P. tauri* (ON220582), were retrieved from GenBank. The sequence from *Nannochloris* sp. '*desiccata*' was obtained from Phycocosm (https://phycocosm.jgi.doe.gov/phycocosm/home). Sequence alignment with ClustalW is available in the project-specific Data Repository, at https://data.mendeley.com/datasets/pfd4g6ts72/2. The 18S phylogeny was inferred using the Maximum Likelihood method and General Time Reversible model of nucleotide substitutions (Nei and Kumar 2000). The initial tree for the heuristic search was selected by choosing the tree with the superior log-likelihood between a Neighbour-Joining (NJ) tree (Saitou and Nei 1987) and a Maximum Parsimony (MP) tree. The NJ tree was generated using a matrix of pairwise distances computed using the General Time Reversible model. The evolutionary rate differences among sites were modelled using a discrete Gamma distribution across five categories (+G, parameter = 0.4062), with 25.63% of sites deemed evolutionarily invariant (+I). The analytical procedure encompassed 26 nucleotide sequences with 5666 positions in the final dataset. Evolutionary analyses were conducted in MEGA12 (Kumar et al. 2024) utilising up to three parallel computing threads.

2.6 | Genome Sequencing and De Novo Assembly

Total DNA was extracted from flash-frozen algal pellets, obtained by centrifugation of 4-L cultures at 3000 *g* for 30 min at RT. Cells were lysed using cetyltrimethylammonium bromide (CTAB), and DNA was extracted using a phenol/chloroform approach as described in Lacroux et al. (2022). Illumina and Pacific Biosciences (PacBio) library preparation and sequencing were performed by Macrogen Inc. (Seoul, South Korea). Illumina libraries were prepared using TruSeq Nano DNA Library Preparation Kit (550) and Illumina platform (2×150-bp paired-end reads). Quality of Illumina raw sequence data was assessed using FastQC software, version 0.11.5 (Andrews 2010). PacBio libraries were made using the SMRTbell template preparation kit with a molecular size cutoff of 10 kb. After reviewing the FastQC report, sequences were trimmed using the software Trimmomatic (Bolger et al. 2014) version 0.39 in accordance with the software manual, setting minimum quality to 25 and minimum length to 35. Trimmed sequences were re-analysed with FastQC to verify the improved data quality. Using the trimmed Illumina reads, the distribution and frequency of kmers were estimated for the library using Jellyfish counts (v 2.3.0) (Marçais and Kingsford 2011), setting the length of kmers to 21. GenomeScope (v2) (Vurture et al. 2017) was used to analyse k-mer frequency distributions, to infer genome size and ploidy and to graphically represent the results. PacBio sequences were used to produce two draft de novo genome assemblies using Canu, version 2.2 (Koren et al. 2017) and Masurca, version 4.0.1 (Kolmogorov et al. 2019). Both draft assemblies were subjected to a Redundans run, version 1.01 (Pryszcz and Gabaldón 2016), to remove redundant contigs, perform the scaffolding and close the gaps in the genome draft assembly. Illumina sequences were used to perform the scaffolding and the gap closing in the Redundans analysis. The two reduced assemblies were merged using quickmerge, version 1.0 (Chakraborty et al. 2016) in order to improve the contiguity of the final assembly. Since the merged assembly still presented a high number of duplications, we performed a final correction process with purge_dups, version 1.2.6 (Guan et al. 2020), that purged haplotigs and overlaps in an assembly based on read depth. Illumina reads were then mapped on the newly produced assembly using Bowtie2, version 2.5 (https://github.com/BenLangmead/bowtie2/), followed by the error correction through the Pilon algorithm, version 1.24 (Walker et al. 2014). Quality and accuracy of the final assembly were evaluated using Quast, version 5.2.0 (Gurevich et al. 2013) and BUSCO, version 5.4.4 (Simão et al. 2015), respectively. To identify segmental duplication in the genome, the software ASGART version 2.4.0 (Delehelle et al. 2018) was used. Gap size was set to 3000 bp, while the minimum length of sequences was set to 5000 bp. The chord plot was produced by setting the minimal identity rate of duplication to 0.9. To evaluate the overlap between the segmental duplication and the coding genes, bedtools intersect, version 2.30.0 (Quinlan and Hall 2010) was used, setting the minimum overlap between the duplicated region and the gene annotation to 10%. Methods used for chloroplast and mitochondrial assembly, annotation and visualisation are described in Supporting Information S1: Method S1.

2.7 | Gene Annotation

Braker2, version 2.1.5 (Hoff et al. 2019), is a fully automated method that uses genomic data to generate full gene structure annotations for novel genomes. It is composed of GeneMark (Brůna et al. 2020) and AUGUSTUS (Stanke et al. 2006). For this analysis, Braker2 was run using the softmasked final assembly. The genome softmasking was performed by EDTA, version 2.0.0 (https://github.com/oushujun/EDTA). Annotation produced by Braker2 and the AUGUSTUS training parameters (-species) were used as input for the gene annotation performed by Maker2 (Holt and Yandell 2011), using reviewed closely related proteins from Uniprot of '*Viridiplantae*' (February 2023) in order to improve the accuracy of the annotation. Produced gene annotation was analysed using BUSCO on both '*Eukaryota*' and '*Chlorophyta*' lineages to evaluate the accuracy of the proteome. Protein sequences were functionally annotated with Trinotate using the revised Viridiplantae proteins from UniProt and the databases downloaded from the Trinotate official website (Griffith et al. 2015).

2.8 | Phylogenomics

To characterise the phylogenetic history of the isolated alga strain within the Chlorophyta, an analysis of orthogroups (OGs) and the birth/death of gene families was performed with OrthoFinder (Emms and Kelly 2019). Only fully annotated *Chlorophyta* genomes (Table S3) were used. OrthoFinder was run on the protein sequences with the following settings: multisequence alignment (MSA) for gene tree inference, diamond_ultra_sens for sequence search, and raxml-ng as a tree inference

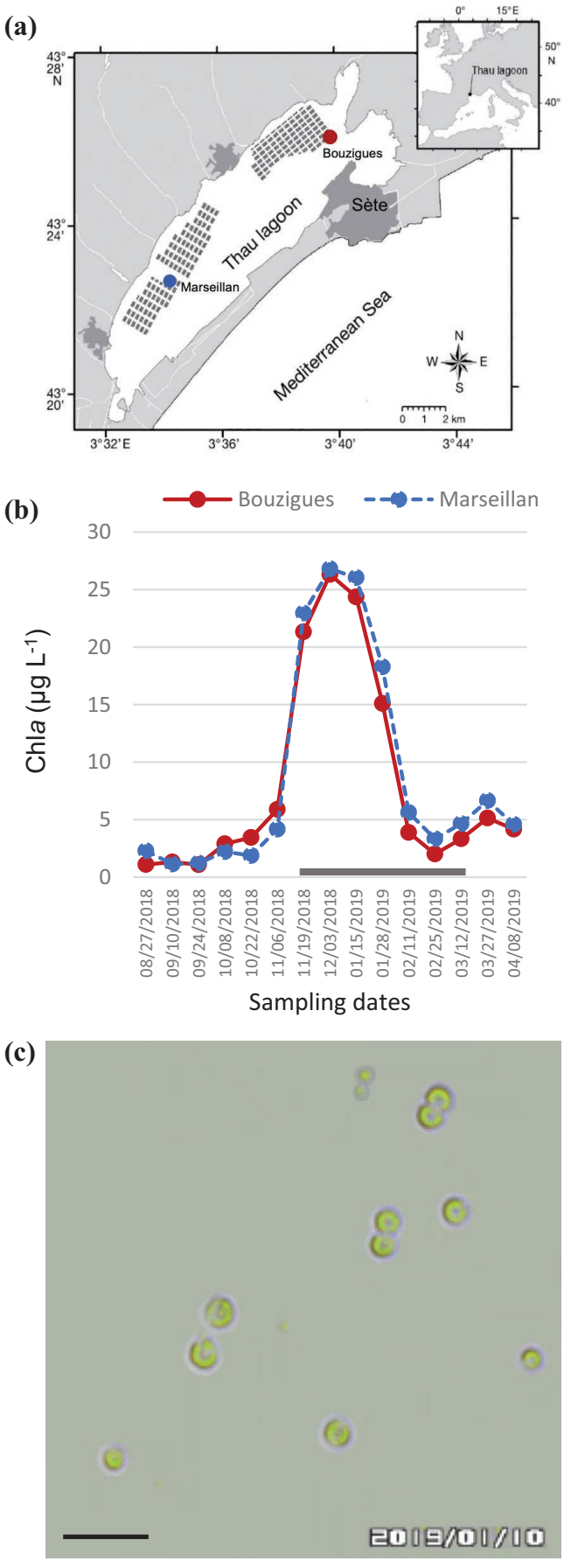

FIGURE 1 | A prolonged winter bloom in the Mediterranean Thau lagoon. (a) Geographical location and sampling sites. (b) Temporal variations of Chl*a* from August 2018 to April 2019 in samples collected in the two relevant sites. Environmental data obtained throughout the autumn and the winter (grey bar) are presented in Figure S1 and Table S1. (c) Representative light micrograph of water samples collected on 10 January 2019. Scale bar: 10 µm.

program, using default parameters. A species tree in Newick format has been visualised with the web tool iTol (Letunic and Bork 2021). The OrthoFinder results are available in the project-specific Data Repository, at https://data.mendeley.com/datasets/pfd4g6ts72/2. For the OrthoFinder analysis using as input only Trebouxiophyceae, the default settings of the tool were also used. Gene Families Birth/Death analysis was performed with the CAFE4 pipeline.

2.9 | In Silico Approach to Protein Identification, Manual Curation and Annotation

The search for specific enzymes and metabolisms was carried out by BLASTp using as queries proteins from the green algae *Chlamydomonas reinhardtii* (https://phytozome-next.jgi.doe.gov/blast-search) and *Chlorella sorokiniana* UTEX 1230 (https://phycocosm.jgi.doe.gov/Chloso1230_1_1/Chloso1230_1_1.home.html), the plant *Arabidopsis thaliana* (https://www.arabidopsis.org/search/protein), and the yeast *Saccharomyces cerevisiae* (https://www.yeastgenome.org/), using default parameters. BLASTp searches for *P. tauri* were performed at https://lobosphaera.ibpc.fr/cgi-bin/AlgoBLAST/algoBlast_mainpage.php, and for other green algae at their respective genome portals (Table S3). Sequences were verified by multiple sequence alignments using Clustal Omega (https://www.ebi.ac.uk/jdispatcher/msa/clustalo), InterPro analyses (https://www.ebi.ac.uk/interpro/) and NCBI_Conserved_Domain (https://www.ncbi.nlm.nih.gov/Structure/cdd/wrpsb.cgi). The database Kyoto Encyclopedia of Genes and Genomes (KEGG) (https://www.genome.jp/kegg/) (Kanehisa et al. 2022) was used for protein family annotation, KEGG Orthology (KO) identification and metabolic pathway reconstruction. Prediction of subcellular localisation of the proteins involved in carbon-concentrating mechanisms (CCMs) was done using DeepLoc-2.1 (https://services.healthtech.dtu.dk/services/DeepLoc-2.1/) (Almagro Armenteros et al. 2017).

3 | Results

3.1 | Identification of the Species Responsible for a Winter Algal Bloom in the Thau Lagoon

The Thau lagoon, one of the largest lagoons on the French Mediterranean coast (Figure 1a), is well known for its shellfish productivity and farming activity. In November 2018, the lagoon waters turned green and remained coloured until the

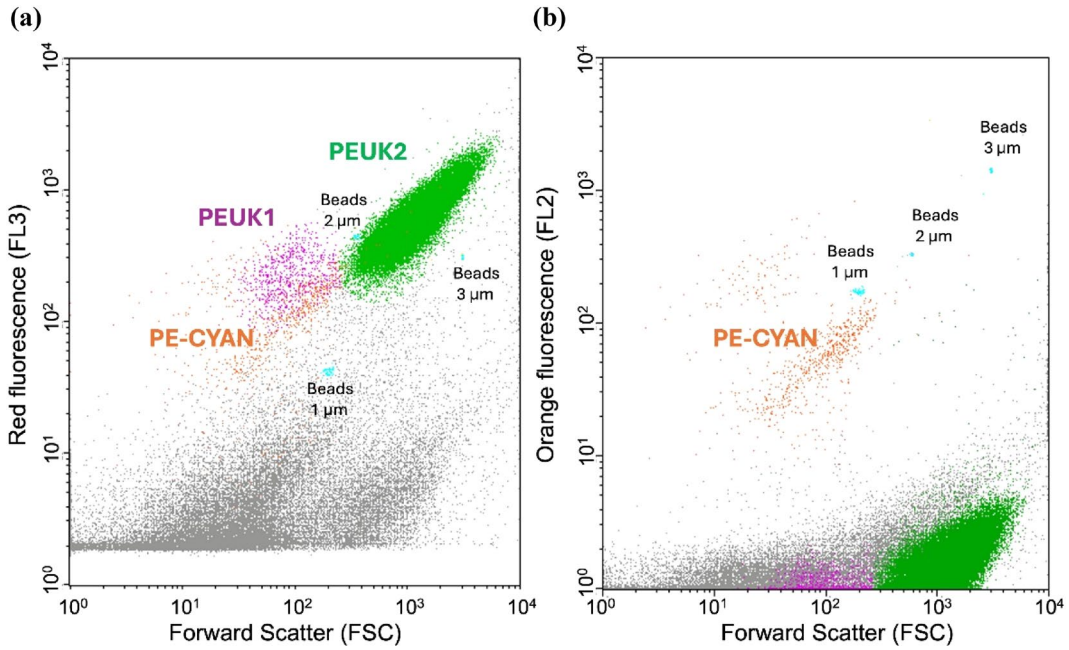

FIGURE 2 | Dot plots of flow cytometry analysis of phytoplankton from water sample collected on 7 January 2019 in the Thau lagoon (site of Bouzigues). Representative plots show (a) Forward scatter vs. red fluorescence and (b) Forward scatter vs orange fluorescence. These dot plots allow discrimination of picocyanobacteria (PE-CYAN) and autotrophic picoeukaryotes (PEUK1 < 1 µm, PEUK2: 2–3 µm).

end of January 2019. A survey of Chl*a* concentrations in surface waters revealed a sharp increase from typical concentrations of 1–2 µg L^{-1} in September 2018 to 26.3 µg L^{-1} in December 2018. Chl*a* concentration remained above 20 µg L^{-1} until mid-January, and then dropped below 5 µg L^{-1} within 2 weeks (Figure 1b). The phytoplankton bloom developed throughout the month of November in rather cool waters (11.3°C–14.9°C) with a daylight period of approximately 9–10 h and an average salinity of 36 (Table S1). The cumulative solar radiation averaged 800 J cm^{-2} (Figure S1). Microscopic observations of samples taken in December 2018 and January 2019 at the sites of Bouzigues and Marseillan indicated the predominance of non-flagellated coccoid green cells with a diameter of 1.5–3 µm (Figure 1c). Flow cytometry analyses indicated the predominance of photosynthetic eukaryotes of small size (< 3 µm). From 17 December 2018 to 26 January 2019, the PPE abundances in surface waters at the site of Bouzigues averaged 10^9 cells L^{-1} (PEUK; Table S1). Of the two major eukaryotic populations identified in January 2019, PEUK1 (1 µm) and PEUK2 (2–3 µm), the latter was by far the most abundant (Figure 2).

A metabarcoding study targeting eukaryotic microbial communities was initiated in December 2018. Within the unicellular photosynthetic eukaryotes, the predominant lineages detected were from two major supergroups, that is, the Archaeplastida and the TSAR (with the Alveolata and Stramenopiles divisions). On 6 December 2018 and 7 January 2019, when Chl*a* levels were at their highest, the sequences stemming from photosynthetic cells were predominantly from the Chlorophyta division (Archaeplastida), representing respectively 67% and 48% of all the sequences (Figure 3), while those from the Alveolata and Stramenopiles together represented 21% and 37.5%. In February, a substantial drop in the Chlorophyta sequences was observed, which represented between 17% and 25% of all sequences. In contrast, the sequences for Alveolata and Stramenopiles increased to 40% on 11 February 2019, and up to 79% on 26 February 2019 (Figure 3, Table S4). In December 2018, the genus *Picochlorum* (Chlorophyta, Trebouxiophyceae) predominated, with 63% of all sequences. The abundance of the genus *Picochlorum* then decreased to 41.9% in January and to less than 3% in February (Figure 3, Tables S4 and S5). Other Chlorophyta identified by the approach were from PPE genera well-known in the Thau lagoon, that is, *Bathycoccus*, *Micromonas* and *Ostreococcus* (Chrétiennot-Dinet and Courties 1997), which all belong to the Mamiellophyceae class. During the period surveyed, *Bathycoccus* represented at most 18.5% of all microbial sequences (26 February 2019), *Micromonas* 2.6% (11 February 2019) and *Ostreococcus* 0.3% (11 February 2019) (Figure 3, Table S5).

From water samples collected early January 2019 at the site of Bouzigues, a small non-flagellated spherical alga representative of the most abundant cells (Figure 1c) was isolated as a monostrain and further cultivated in axenic conditions. Phylogeny of the 18S ribosomal gene sequence indicated that the isolated alga belonged to the *Picochlorum* clade and was distinct from already described Mediterranean species (Figure 4). The closest sequence homologue was from *Picochlorum* sp. CTM20019 isolated from Tunisian waters, with 99.7% sequence identity (1764/1768) (Figure 4). *P. costavermella*, which was isolated at the estuary of the French coastal river 'La Massane' (near Banyuls, South west of the Thau lagoon, France) (Krasovec et al. 2018), appeared more distant. TEM pictures revealed that the algal cells had a size ranging from 1.5 to 3 µm, contained one chloroplast and one mitochondrion, and divided by autosporulation (Figure 5). In the chloroplast, small starch grains were observed squeezed between thylakoids. Within the starch granules, no obvious pyrenoid could be observed, which contrasts

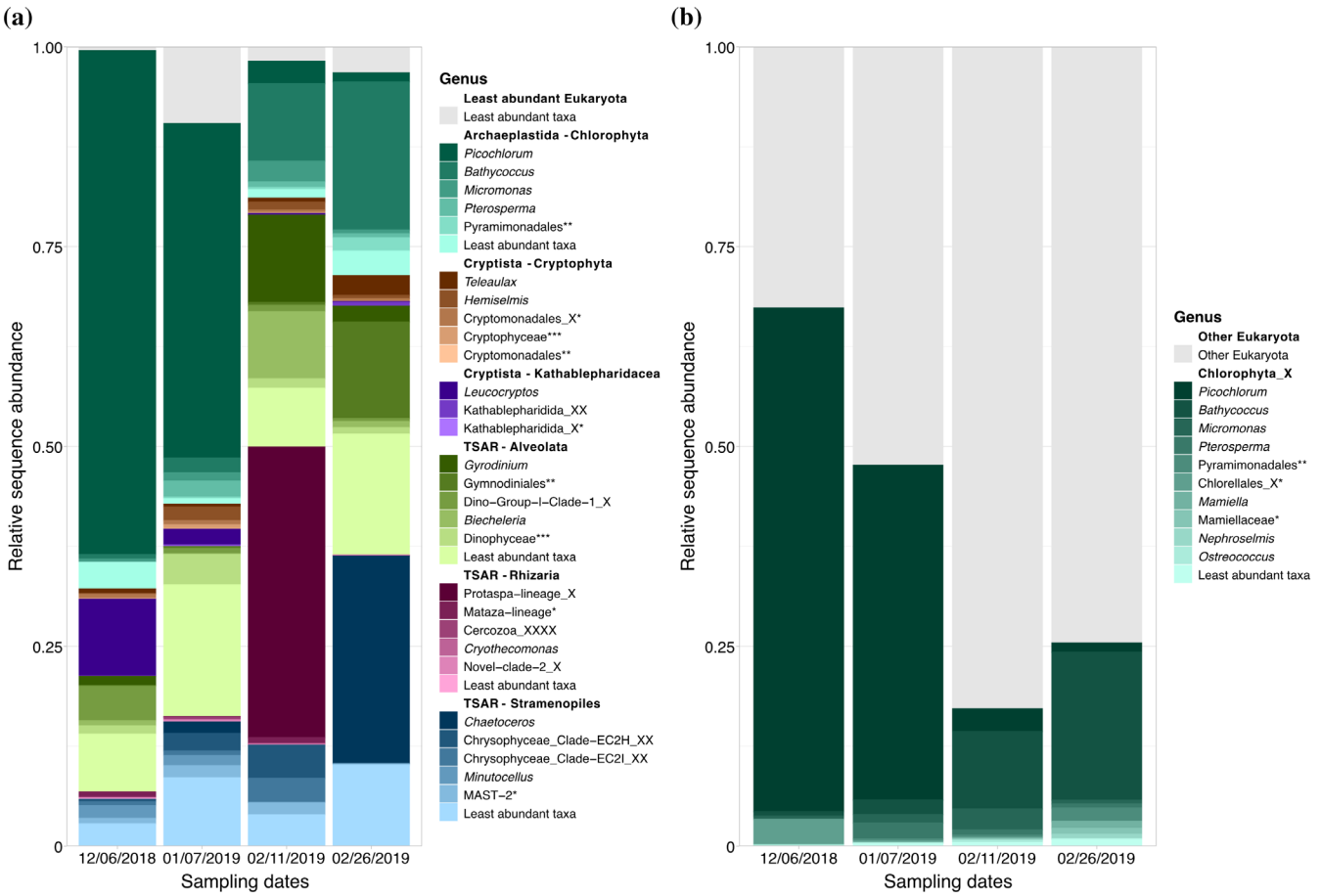

FIGURE 3 | Taxonomic diversity and distribution of eukaryotic microbial communities in the water column at the surface of the Bouzigues site from December 2018 to February 2019. (a) The six most abundant Divisions were represented and classified by Supergroup. The five most abundant genera within a Division were ordered from the most to the least abundant. (b) The 10 most abundant genera within the Chlorophyta division were ordered from the most to the least abundant. Sequences from microbial Eukaryota that were not identified as Chlorophyta_X were summed and represented as 'Other Eukaryota'. In both panels, less abundant genera were summed and represented as 'Least abundant taxa'. Taxonomic groups with a name ending with at least a* were not taxonomically identified to the represented taxonomic level using the PR2 database. Taxonomic groups with a name ending with at least a _X were created by PR2 taxonomic experts to homogenise the taxonomic classification.

with the situation in most trebouxiophyceans (Luo et al. 2010). Studies indicated that the isolated alga is able to grow in the absence of added vitamins (Figure 6). Supplementation of the growth medium with a mix of B-vitamins (B1, B7 and B12) did not boost the algal growth (Figure 6). From 18S rDNA phylogeny (Figure 4) and phylogenomics (see below), it was inferred that the alga isolated from the Mediterranean Thau lagoon represented an undescribed species in the *Picochlorum* genus. It was then named *P. tauri*.

3.2 | *P. tauri* Hemon & Grimsley, sp. nov.

3.2.1 | Description

Small coccoid single cell with a diameter of 1.5–3 μm. A cell contains one chloroplast and one mitochondrion. Chloroplast pigments include chlorophylls *a* and *b*. Starch grains present. Flagella and pyrenoid are absent. Reproduction by autosporulation. Representative illustration: optical and electron microscopy (Figures 1c and 5). Does not require exogenous vitamins for growth. The genome is 13.6 Mb in length and contains 6636 protein-coding genes.

3.2.2 | Diagnosis

Differs from other *Picochlorum* species through genetic signatures in 18S rDNA (GenBank: ON220582). The closest sequence is that of *Picochlorum* CTM200019, for which no genome sequence data is currently available. *P. tauri* has five identical 18S rRNA gene copies, representing the largest gene set among the genome-sequenced *Picochlorum* species (Table S6). Phylogenomics indicates a close proximity to *Picochlorum* BPE23 (Bonaire) and *Picochlorum* SENEW3 (San Elijo Lagoon estuary).

3.2.3 | Holotype

The authentic strain is preserved on paper at the Muséum National d'Histoire Naturelle (MNHN, Paris, France) under the number PC0683151.

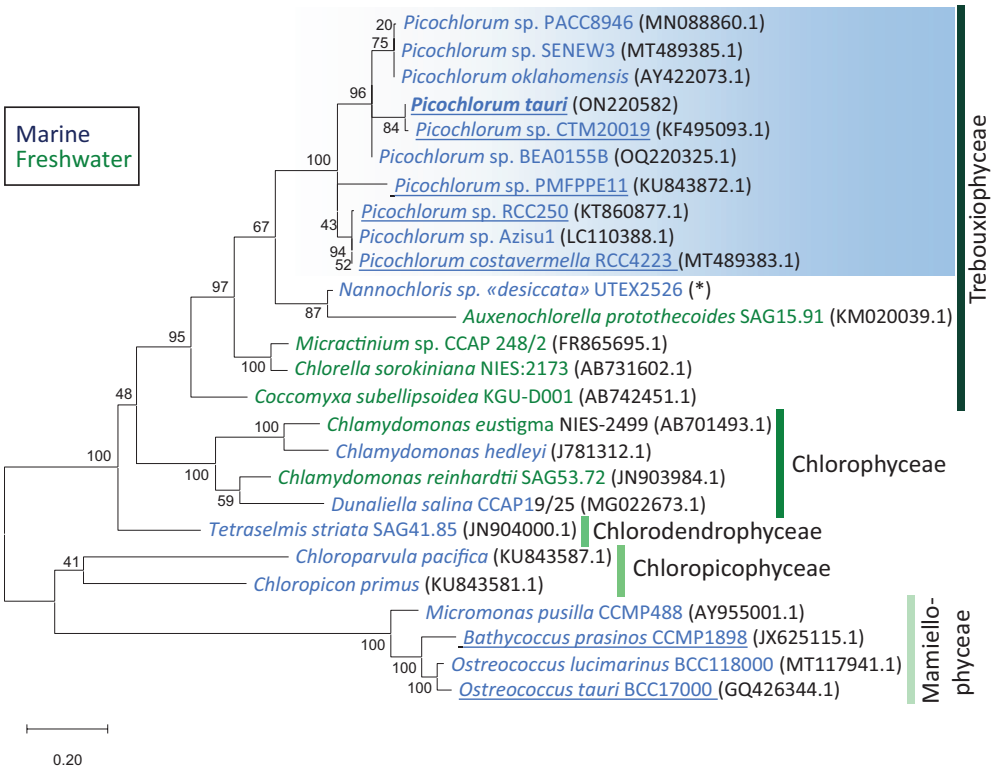

FIGURE 4 | Molecular phylogeny based on 18S rDNA sequence comparison. The phylogeny was inferred using the Maximum Likelihood method and the General Time Reversible model of nucleotide substitutions. The evolutionary rate differences among sites were modelled using a discrete Gamma distribution across five categories (+G, parameter = 0.4062), with 25.63% of sites deemed evolutionarily invariant (+I). Branch lengths represent substitutions per site. The percentage of replicate trees in which the associated taxa clustered together (100 replicates) is shown next to the branches. The analytical procedure encompassed 26 nucleotide sequences with 5666 positions in the final dataset. Mediterranean species are underlined. The *Picochlorum* clade is highlighted in blue.

3.2.4 | Geographic Distribution

Shellfish farming site of Bouzigues in the Thau Lagoon, France (GPS WGS84 coordinates: Long 3.66463°E, Lat 43.43429°N). Isolated from the surface water (1 m depth) in January 2019.

3.2.5 | Reference Material

Living culture is maintained in artificial seawater (f/2 medium, PiF medium). It is available at MARBEC, Sète, France.

3.2.6 | Etymology

The species epithet 'tauri' is based on the type locality. Thau comes from an old pre-Indo-European hydronymic radical 'taur-', meaning 'water' (Hamlin 1988).

3.3 | *P. tauri* Genome Sequencing and Assembly Showing Typical Compactness

Using a combination of 69,398,852 short sequence reads (Illumina) and 673,627 long sequence reads (Pacific Biosciences), the nuclear and organelle genome sequences of *P. tauri* were assembled. The nuclear genome was assembled into 27 contigs with a total length of 13,627,862 bp, with an N50 value of 984,432 bp, an L50 value of 6 and a N90 value of 294,601 bp (Tables S7 and S8). The nuclear genome assembly had no gaps (N's) and G + C content of 46.11%. The GenomeScope analysis estimated the genome size to be 12,693,064 bp, with heterozygosity estimated at 0.575% (Figure S2), thus suggesting that the sequenced strain is diploid. The Benchmarking Universal Single-Copy Orthologs (BUSCO) analysis using *Eukaryota* as reference lineage resulted in 84.3% complete BUSCOs (83.9% as single copy, 0.4% as duplicate), 3.1% fragmented and 12.6% missing. BUSCO analysis using *Chlorophyta* as reference lineage resulted in 94.5% of the BUSCOs identified as complete (93.7% in single copy, 0.8% in duplicate), 0.9% as fragmented and 4.6% missing (Figure S3). Altogether, these data indicated a high level of completeness of the nuclear genome assembly. From the Illumina and PacBio sequences, the chloroplast and mitochondrial genome sequences were assembled with a 674-fold coverage and 379-fold coverage, respectively (Table S7). The chloroplast genome (ptDNA) of *P. tauri* is a circular molecule of 74,276 bp (Figure S4), with a G + C content of 32%, in line with trebouxiophycean plastid genomes (Table S9). The *P. tauri* mitochondrial DNA (mtDNA) is a circular 35,605 bp long genome (Figure S5). Its G + C content of 42.46% is in stark contrast with that of mtDNA of most trebouxiophyceans and other green algae, in which it is on average 25%–28% (Smith et al. 2011) (Table S10). The total number of protein-encoding genes predicted from the obtained sequence assemblies was 6636 for the nuclear genome, 76 for the ptDNA, and 33 for the mtDNA genome (Tables S9 and S10).

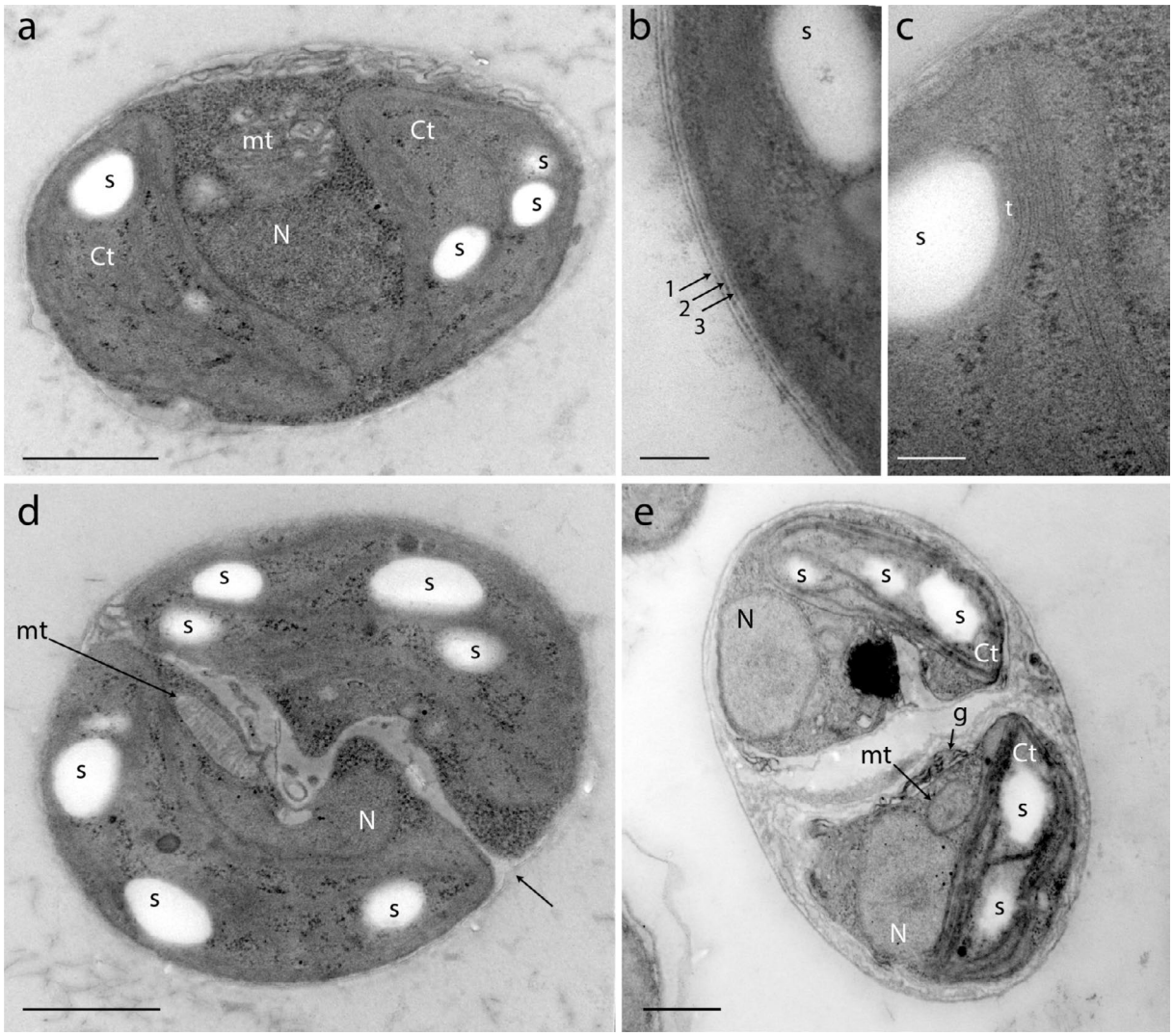

FIGURE 5 | Transmission electron micrographs of *Picochlorum tauri*. Cells have a round or ovoid shape. The nucleus is in the centre of the cell, covered by the chloroplast. The mitochondria often appear with an electron-dense matrix. Starch grains are numerous and appear with no obvious pyrenoid. The thylakoid membranes appear as dark lines, as in panel (c). Ct, chloroplast; g, golgi; mt, mitochondria; N, nucleus; S, starch grain; T, thylakoids. Panel (d) shows the arrow pointing at the V-shape invagination of the cell wall in a dividing cell. Scale bars: (a, d, e) 0.5 μm; (b, c) 0.1 μm.

3.4 | Phylogenomics and Genome Evolution Among Trebouxiophyceae

An OG analysis using 43 primary plastid-bearing algae with full-length sequenced genomes was performed to position the newly isolated alga species within the Chlorophyta. The analysis was run with the OrthoFinder pipeline (Emms and Kelly 2019), which integrates information from OGs. A species tree was inferred from the set of unrooted OG gene trees using the STAG method as implemented in OrthoFinder (Figure 7). The phylogenomic analysis placed *P. tauri* within the *Picochlorum* genus in the Trebouxiophyceae class (Figure 7) and suggested that *P. tauri* is most similar to *Picochlorum* SENEW3, isolated from a poikilohaline pond in the San Elijo Lagoon estuary (California) (Wang et al. 2014; Foflonker et al. 2015) and *Picochlorum* BPE23, isolated from a lagoon at Bonaire (Caribbean Sea) (Barten et al. 2022). Like the other members of the *Picochlorum* genus (Table S11), *P. tauri* is characterised by a small genome and protein repertoires (Figure 7).

To shed light on the reduced genome and proteome sizes in *P. tauri* with respect to other trebouxiophyceans (Figure 7), we first focused on the organellar genomes. The gene repertoires in *P. tauri* mitochondrial and chloroplast genomes were compared to trebouxiophyceans selected for their distinct habitat and physiology, namely the photosynthetic freshwater species *Chlorella sorokiniana* (*C. sorokiniana*), *Auxenochlorella protothecoides* (*A. protothecoides*) and *Coccomyxae subellipsoida* (*C. subellipsoida*), and the non-photosynthetic obligate parasites *Prototheca wickerhamii* (*P. wickerhamii*) and *Helicosporidium* sp. The *P. tauri* ptDNA gene set appeared quite comparable to that of other trebouxiophyceans (Table S9) (Turmel et al. 2015). Indeed, in *P. tauri* ptDNA, a total of 108 conserved genes were identified, including 36 genes for proteins involved in photosynthesis, 21 for subunits of the chloroplast ribosome, 3 ribosomal RNA genes (rrn23, rrn16 and rrn5) and 29 tRNA-encoding genes. Similar to the other trebouxiophyceans, *P. tauri*'s ptDNA genome had *chlB*, *chlN* and *chlL* coding for the three subunits of the dark-active protochlorophyllide (PChlide) oxidoreductase (D-POR), which reduces PChlide

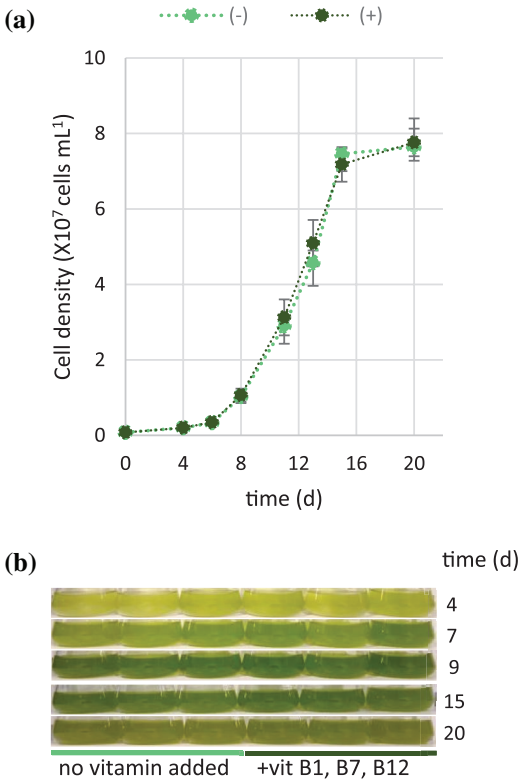

FIGURE 6 | Effect of exogenous vitamins on *Picochlorum tauri* growth. Algae were cultivated with (+) or without (–) added vitamins B1, B7 and B12, at 22°C under a 14 h:10 h light:dark cycle (light intensity of 100 μmol photons $m^{-2}s^{-1}$). (a) Growth curves. Error bars indicate SDs based on three independent biological replicates per condition. (b) Overview of the cultures over 20 days.

ring D into Chlorophyllide *a* (Armstrong 1998). It was noted that in contrast to the other (photosynthetic) trebouxiophyceans surveyed (Table S9; Turmel et al. 2015), *P. tauri* ptDNA lacked the *cysA* and *cysT* genes, which code for subunits of the chloroplast sulfate anion transport complex (cysATW). The gene repertoire in *P. tauri* mtDNA was highly comparable to that found in other trebouxiophyceans (Table S10). A total of 59 putative genes were identified, consisting of 23 transfer RNA (tRNA)-encoding genes, 3 ribosomal RNA genes, 18 genes coding for subunits of the respiratory chain and the ATP synthase and 14 genes for ribosomal proteins (Table S10). In addition, *P. tauri* mtDNA had a *tatC* gene, potentially coding for a component of the protein export TAT pathway, which exclusively translocates fully folded or even multi-subunit complexes across the mitochondrial inner membrane (Palmer and Stansfeld 2020).

The nuclear protein-coding gene content of *P. tauri* was analysed in the light of its relatives in the genus *Picochlorum* and other trebouxiophycean genera with fully sequenced genomes. The OrthoFinder software was run with predicted proteomes of *P. tauri* and the eight *Picochlorum* species isolated from different geographical locations (Table S11), and of five members of the *Chlorella* clade (*C. sorokiniana*, *C. vulgaris*, *C. ohadii*, *A. prothotecoides* and *Helicosporidium*), two members of the *Coccomyxa* clade (*C. subellipsoida* and *C. obi*) and one member of the *Nannochloris* clade (*N. desiccata*, formerly called *Chlorella desiccata*) (Sanders et al. 2022) (Table S1). In the analysis, a total of 13,846 OGs were defined, of which 3619 (26%) were shared by all *Picochlorum* species (OrthoFinder results at https://data.mendeley.com/datasets/pfd4g6ts72/2). The rooted species tree revealed the loss of 196 OGs on the *Picochlorum* branch (Figure S6).

3.5 | Carbon Metabolism in *P. tauri* and Its Relatives Within the Trebouxiophyceae Class

The predominant mechanism for carbon fixation in photosynthetic cells is the Calvin–Benson–Bassham (CBB) reductive pentose phosphate pathway (Tabita 1999). The key enzyme of this cycle is the ribulose-1,5-bisphosphate carboxylase/oxygenase (RubisCO; EC 4.1.1.39), a hexadecameric complex of 550 kDa made up of eight copies of both large (catalytic) (RBCL) and small (RBCS) subunits (Knight et al. 1990). *P. tauri* contained one *rbcL* gene copy (ptDNA) and three copies of *RBCS* (nDNA) (Table S12), being the highest copy number in the *Picochlorum* spp. (Figure 8). Under high carbon dioxide (CO_2), RubisCO acts as a carboxylase, fixing CO_2 into ribulose-1,5-bisphosphate (Figure 9a). Under low CO_2, the enzyme functions as an oxygenase and evolves phosphoglycolate, which is recycled via the photorespiratory pathway. The enzymes of this pathway are: a glycolate oxidase, a serine/glycine hydroxymethyltransferase, and a D-glycerate 3-kinase (Figure 8). The RubisCO operating efficiency can be enhanced by CCMs, which increase the CO_2 concentration to a level that nearly saturates the enzyme active site (Giordano et al. 2005; Reinfelder 2011). As inferred by our genome survey, *P. tauri* possesses genes for both biochemical (CO_2 fixation prior to RubisCO) and biophysical (increasing HCO_3^- inside the cell) CCMs. We identified in *P. tauri* one gene for a phosphoenolpyruvate carboxylase (PEPC; EC 4.1.1.31), an enzyme that catalyses the formation of the four-carbon acid compound oxaloacetate (OAA) through the carboxylation of phosphoenolpyruvate (PEP) (Figure 9a), which has a higher affinity for CO_2 (specifically HCO_3^-) than RubisCO and does not use O_2. All *Picochlorum* spp. but NBRC102739 were found to have one PEPC gene copy, contrasting with the other trebouxiophycean species, which have two copies (Figure 8). It was inferred that *P. tauri* can reduce OAA to malate as a gene for malate dehydrogenase (MDH; EC 1.1.1.37) was identified (Figures 8 and 9a). Genes for two decarboxylating enzymes potentially delivering CO_2 to RubisCO were identified in *P. tauri*: (i) a phosphoenolpyruvate carboxykinase (ATP) (PCK; EC 4.1.1.49) for the decarboxylation of OAA to PEP; and (ii) a NADP-malic enzyme (ME; EC 1.1.1.40) that produces pyruvate from malate (Figures 8 and 9a). The presence in *P. tauri* of a pyruvate orthophosphate dikinase (PPDK; EC 2.7.9.1) indicates that pyruvate (stemming from ME) can be activated into PEP. Biophysical CCM includes inorganic carbon transporters and carbonic anhydrases (CA; EC 4.2.1.1). A homologue of the solute carrier SLC4, involved in the direct HCO_3^- uptake in diatoms (Tsuji et al. 2017), was identified in *P. tauri* (Table S12; Figure 8). CAs catalyse the CO_2/HCO_3^- interconversion, allowing an increase in bicarbonate inside the cell and its subsequent conversion to CO_2 in close proximity to RubisCO (Giordano et al. 2005; Meyer and Griffiths 2013). In the genome of *P. tauri*, two α-CA genes, one β-CA gene and

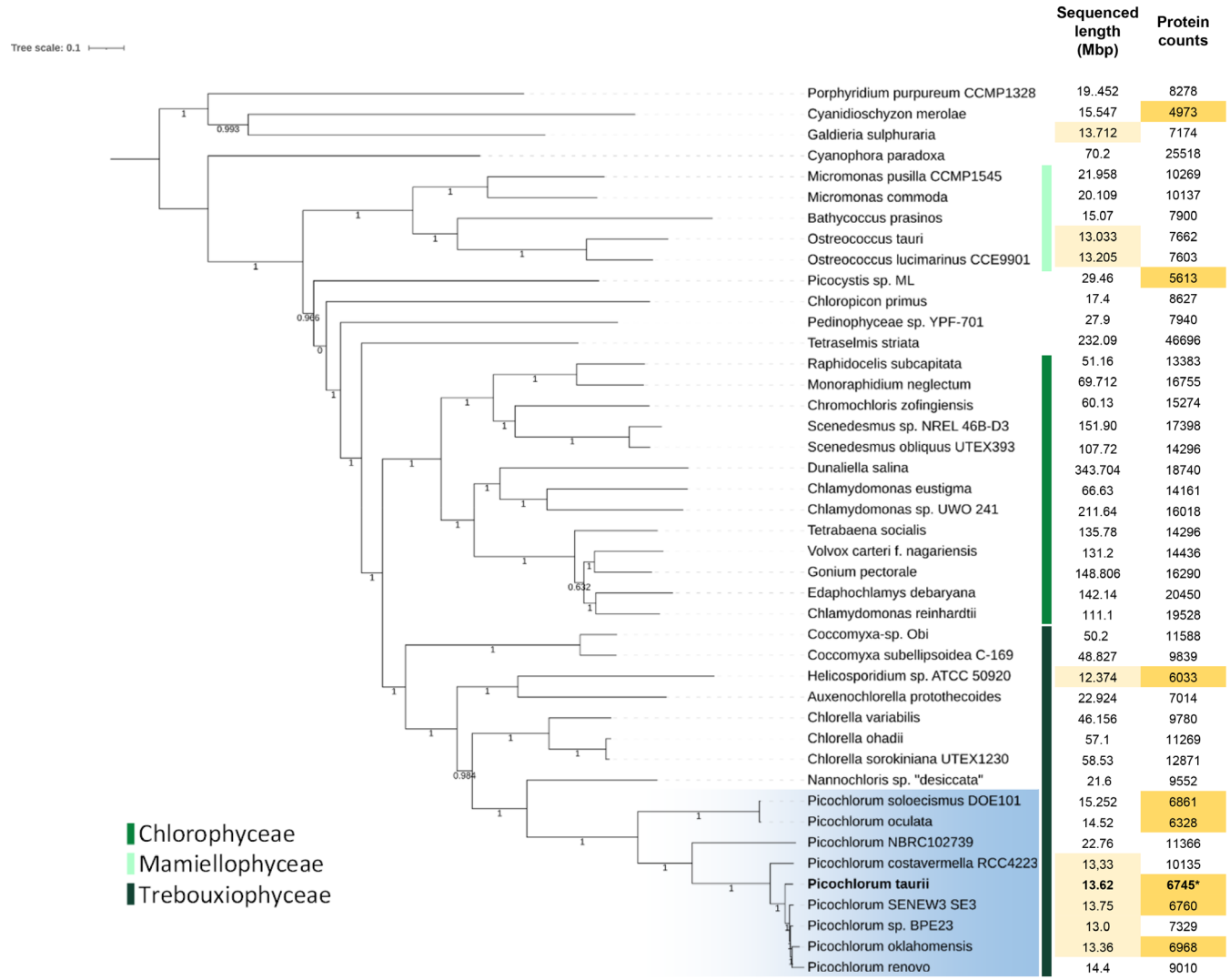

FIGURE 7 | Phylogenomic tree including 43 Chlorophyta algal genomes. OrthoFinder was run on protein sequences with the following settings: MSA for the gene tree inference, diamond_ultra_sens for the sequence search and raxml-ng as a tree inference program. A species tree was inferred from the set of unrooted orthogroup gene trees using the STAG method as implemented in OrthoFinder. STAG support values are indicated at the nodes. The *Picochlorum* clade is highlighted in blue. Respective genome (assemblies) and protein repertoire sizes are indicated. Protein counts refer to the entire set of protein-coding genes available from each genome database (Table S2). Highlighted in yellow are the smallest genome sequences (< 14 Mbp); in orange are the smallest predicted proteomes (< 7000 protein counts).

three γ-CA genes were detected (Figure 8). The gene copies for α-CA and β-CA, likely components of the CCM, appeared reduced in *P. tauri* and other *Picochlorum* spp. as compared to other trebouxiophyceans (Figure 8) and plants (DiMario et al. 2017). Arranged in a module on the mitochondrial respiratory Complex I, γ-CAs are proposed to play a role in mitochondrial metabolism by specifically providing protons at the inside of the inner mitochondrial membrane and thus maintaining a proton gradient (Braun and Klusch 2024).

Acetyl-CoA (AcCoA), a high-energy biosynthetic precursor, represents a central hub in carbon metabolism. AcCoA generation from pyruvate, stemming primarily from the glycolytic pathway, can occur via three distinct enzymatic complexes: (i) a pyruvate dehydrogenase (PDH), (ii) a pyruvate ferredoxin oxidoreductase (PFO; EC 1.2.7.1) or a pyruvate formate lyase (PFL; EC 2.3.1.54). While the first enzyme functions under aerobic conditions, the other two are oxygen-sensitive (Atteia et al. 2013). In *P. tauri*, PDH subunits E1α, E1β, E2 and E3, as well as PDH kinase were identified (Table S12). In contrast, neither *PFL* nor *PFO* was found in *P. tauri* and other *Picochlorum* spp. (Figure 8). Anaerobic production of AcCoA from pyruvate thus appears restricted to few trebouxiophycean species, namely the photosynthetic species of the Chlorella clade, that is, *C. ohadii*, *C. sorokiniana* and *C. variabilis*. AcCoA can be generated from acetate. The most common route involves a single step with an AcCoA synthetase (ACS; EC 6.2.1.1). The number of *ACS* genes varies in other trebouxiophyceans from one (*A. Protothecoides*) up to four (*C. sorokiniana* and *C. ohadii*). All *Picochlorum* species are predicted to have one *ACS* gene copy, except *Picochlorum* NBRC120739, in which two *ACS* genes were found. In bacteria and a few eukaryotes, AcCoA can also be generated from acetate via a two-enzyme route, consisting of an acetate kinase (ACK; EC 2.7.2.15) and a phosphate acetyltransferase (PTA; EC 2.3.1.8). Genes for these

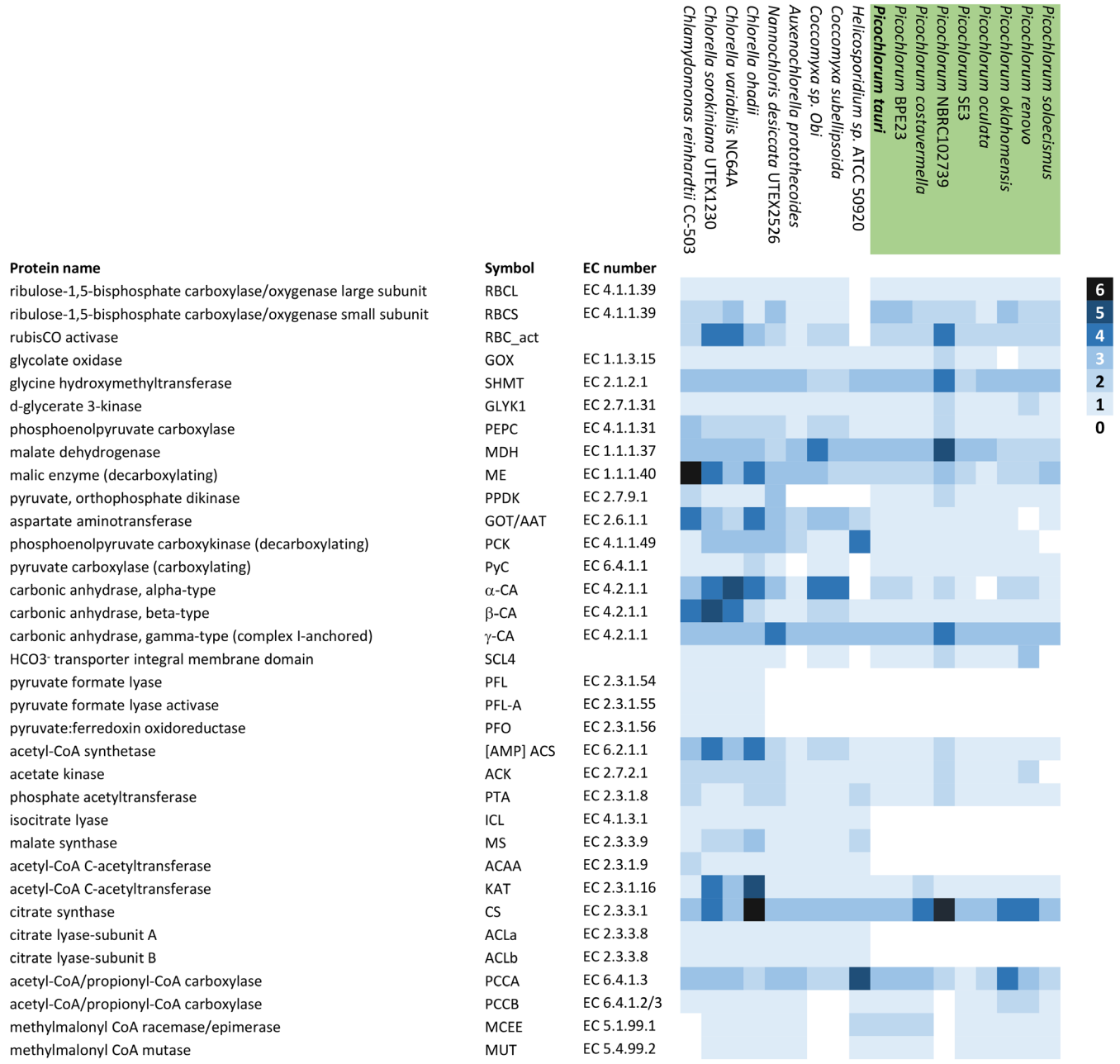

FIGURE 8 | Protein-coding gene content for carbon metabolism across the Trebouxiophyceae diversity. The number of gene copies is colour-coded, ranging from white (absence of gene) to navy blue (six copies). *Picochlorum* spp. are highlighted in green. Accession numbers to predicted proteins are found in Table S12.

enzymes were found in *P. tauri* and other *Picochlorum* spp., apart from *P. soloecismus*, in which *ACK* seems to be missing (Figure 8). In *P. tauri*, the two genes were found on the same contig, separated by one gene encoding a homologue of a phosphate starvation response protein.

The glyoxylate cycle plays an essential role in allowing growth on two-carbon compounds such as acetate and ethanol (Kornberg and Madsen 1957). In addition to three enzymes of the TCA cycle (CS, EC 2.3.3.1; ACO, EC 4.2.1.3; MDH, EC 1.1.1.37), the glyoxylate cycle requires two unique enzymes, an isocitrate lyase (ICL; EC 4.1.3) and a malate synthase (MS; EC 2.3.3.9). The *ICL* and *MS* genes were not found in *P. tauri* and other *Picochlorum* species, contrasting with the other trebouxiophyceans surveyed (Figure 8). AcCoA C-acetyltransferases exist in two distinct forms: one form catalyses the reversible conversion of acetoacetyl-CoA into two molecules of AcCoA (ACAT; EC 2.3.1.9), and another catalyses the thiolytic cleavage of straight-chain 3-keto fatty acyl-CoAs (KAT; EC 2.3.1.16). *P. tauri* and other *Picochlorum* spp. had only one *KAT* gene, in contrast to the other trebouxiophyceans, which had genes for both forms (Figure 8). Citrate synthase (CS; EC 2.3.3.1), which combines AcCoA to OAA, is present in multiple copies in *P. tauri*, thus resembling other trebouxiophyceans (Figure 8). ATP-dependent and CoA-dependent ATP citrate lyase (ACLY; EC 2.3.3.8) is a cytosolic enzyme that catalyses the cleavage of mitochondrially

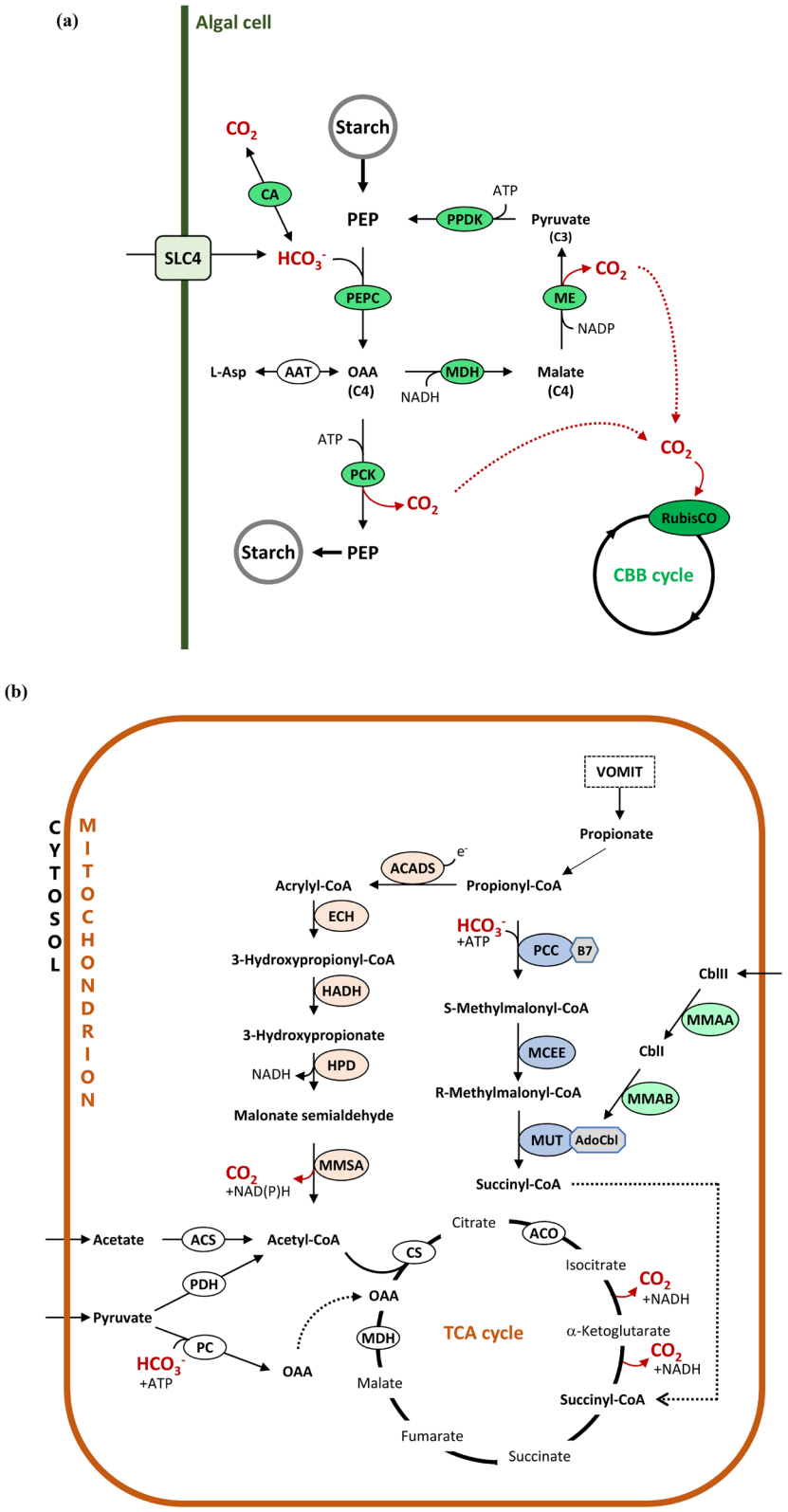

FIGURE 9 | Legend on next page.

exported citrate into AcCoA and OAA. The survey indicated that the genes for ACLY were absent in *P. tauri* and other *Picochlorum* species, while present in all trebouxiophyceans.

Propionyl-CoA, resulting from the catabolism of odd-chain fatty acids, Methionine and branched-chain amino acids (Val, Ile and Thr) (VOMIT), can be converted to AcCoA and CO_2 via a β oxidation-like pathway. All the genes for this pathway were identified in the *P. tauri* genome (Figure 9b). Mining of the *P. tauri* genome uncovered genes for an alternative route for propionate/propionyl-CoA detoxification. This route, called the 'carboxylation pathway' leads to succinyl-CoA (Watson et al. 2016)

FIGURE 9 | Metabolic pathway reconstruction. (a) Carbon concentrating mechanisms in *Picochlorum tauri* as inferred from its genome sequence. Carbonic anhydrases (CA) catalyse the reversible hydration of carbon dioxide (CO_2). The carboxylation of phosphoenolpyruvate (PEP) stemming from glycolysis generates oxaloacetate (OAA), which can then be converted to malate or L-aspartate. CO_2 produced in the decarboxylation reactions (ME and PCK) is subsequently fixed by RubisCO. Enzymes involved in CCMs are indicated in light green-filled ellipses. In higher plants, the enzymes associated with the biochemical CCMs are localised to specific cell compartments and are associated with metabolisms referred to as CAM photosynthesis and C4 photosynthesis (Yamori et al. 2014). In the picoalgae, the enzyme's exact localisation is not known. The multi-label predictor DeepLoc (version 2.1) predicted a chloroplast localisation for PPDK, a mitochondrial localisation for the two MEs, and a cytoplasm localisation for PEPC and PCK. L-Asp, L-aspartate. See Figure 8 for the enzyme full names. (b) Overlap of the TCA cycle and the propionate breakdown pathways in *P. tauri*, as inferred from its genome sequence. Propionyl-CoA is produced during the catabolism of Valine, Odd chain fatty acids, Methionine, Isoleucine and Threonine (VOMIT). The *carboxylation pathway* for propionate breakdown comprises three enzymes, depicted here in blue-coloured ellipses. The *carboxylation pathway* generates succinyl-CoA, a TCA cycle intermediate; bypassing the steps of the TCA cycle that produce CO_2 and NADH, this pathway favours C-conservation over energy conservation. The β oxidation-like pathway for propionate breakdown leads to acetyl-CoA (enzymes depicted in light orange), which favours energy production over C-conservation. ACADS, short-chain specific acyl-CoA dehydrogenase (EC 1.3.8.1); ECH, enoyl-CoA hydratase (EC 4.2.1.17); HADH, 3-hydroxyisobutyryl-CoA hydrolase (EC 3.1.2.4); HPD, 3-hydroxypropionate dehydrogenase (EC 1.1.1.31); MCEE, methylmalonyl-CoA epimerase; MMSA, malonate-semialdehyde dehydrogenase (acetylating) (EC 1.2.1.18); MUT, methylmalonyl-CoA mutase; PC, pyruvate carboxylase; PCC, propionyl-CoA carboxylase; PDH, pyruvate dehydrogenase. Proteins required for the conversion of Cbl into AdoCbl are depicted in light green ellipses: MMAA, methylmalonic aciduria type A protein; MMAB, ATP:Cob(I)alamin adenosyltransferase. Enzyme cofactors derived from vitamins are depicted in grey. Full names and EC numbers of all other enzymes are given in Figures 8 and 10, and in Table S12.

and involves three mitochondrial enzymes: (i) a propionyl-CoA carboxylase (PCC; EC 6.4.1.3) which catalyses the carboxylation of propionyl-CoA with bicarbonate to methylmalonyl-CoA, (ii) a methylmalonyl-CoA epimerase (MCEE; EC 5.1.99.1) and (iii) a methylmalonyl-CoA mutase (MUT; EC 5.4.99.2) which catalyses the adenosylcobalamin (AdoCbl)-dependent rearrangement of methylmalonyl-CoA (mmCoA) to succinyl-CoA (Figure 9b). As revealed here, this route is not universally present among the Trebouxiophyceae: it is missing in the species of the genus *Coccomyxa* and in *Picochlorum* NBRC102739 (Figure 8).

3.6 | Comparative Genomics of Metabolic Specificities of *P. tauri* and Other Marine Photosynthetic Eukaryotes

We conducted a comparative genomic study of *P. tauri* with other PPEs that have fully sequenced genomes, including the mamiellophyceans *Ostreococcus* spp., *Micromonas* spp. and *Bathycoccus prasinos*, the chloropicophycean *Chloropicon primus* and the picocystophycean *Picocystis* ML (Table S13), with a focus on CO_2 fixation, N-acquisition, chlorophyll and vitamin synthesis. Picoalgal genomes were first searched for CCM components. All PPEs, except *Picocystis* ML, have a *PEPC* gene for PEP carboxylation (Figures 9a and 10). All PPEs but *C. primus* have several *ME* genes and one *PPDK* gene. In contrast to *P. tauri*, all five mamiellophyceans lack a *PCK* gene (Figures 9a and 10) (Derelle et al. 2006). Among the PPEs, the gene repertoires for CAs greatly vary, and *P. tauri's* genome showed the highest gene copy number (Figure 10). The smallest CA repertoires were found in *Picocystis* ML, which has one γ-CA, and in *O. tauri* and *O. lucimarinus*, each harbouring one gene for a β-CA and one for a δ-CA (Figure 10). The δ-type CA, seldom distributed among Chlorophyta (DiMario et al. 2018), was not found in *P. tauri*. The survey revealed that the *Picochlorum* spp. are the only PPEs to have *MCEE* and *MUT* genes for the propionyl-CoA carboxylation pathway (Figures 9b and 10).

Nitrogen is an essential macronutrient required for the synthesis of key biomolecules, such as proteins and nucleic acids. Phytoplanktonic species can typically use the two forms of dissolved nitrogen: (i) inorganic nitrogen (DIN) composed of nitrate (NO_3^-) and ammonium (NH_4^+), and (ii) organic nitrogen (DON) consisting primarily of urea, amino acids and nucleic acids. Exchange of NH_4/NH_3 across biological membranes is facilitated by transporters of the ubiquitous Mep/Amt/Rh transporter superfamily (McDonald et al. 2012; Williamson et al. 2024). In plants and microalgae, NH_4-transporters are located in the plasma membrane (for the import inside the cell) and in the chloroplast envelope (for the intracellular transport to the organelle). It is long known that algae of the Mamiellophyceae class have multiple ammonium transporters (from three to six), belonging to the AMT1- and AMT2-types (McDonald et al. 2010). In *C. primus*, four AMT1-type genes have been uncovered, while in *Picocystis* ML, four Rh-type genes were detected. In stark contrast, in *P. tauri*, as well as in the other *Picochlorum* spp., only one gene for a potential AMT1-type transporter was identified (Figures 10, S7 and S8). The *P. tauri* predicted AMT has a typical topology with 11 transmembrane alpha-helical spanners (TMs) but is characterised by a larger domain between TMs 2 and 3 (81 aa vs. 27 in *E. coli* ATMB) with a high content in Cys (4) and Thr (17) residues (Figure S7). Nitrate transporter (NRT) in the plasma membrane can deliver nitrate to the cytosol, where it is reduced to nitrite by nitrate reductase (NR; EC 1.7.1.1). Nitrite is then transported into the chloroplast via a nitrite transporter (NAR1), where it is reduced to ammonium by nitrite reductase (NiR; EC 1.7.7.1) (Fernandez and Galvan 2007). Genome survey showed that all *Picochlorum* spp. have the necessary genes to import nitrate from the environment and reduce it to nitrite (Figure 10). All PPEs but *Picocystis* sp. ML have a formate/nitrite transporter and a nitrite reductase. Urea can be imported from the environment by a high affinity urea-proton transporter (DUR3), and converted to NH4 via two distinct pathways: (i) the one-step pathway catalysed by a urease (URE; EC 3.5.1.5), and (ii) a two-enzyme pathway which involves a urea

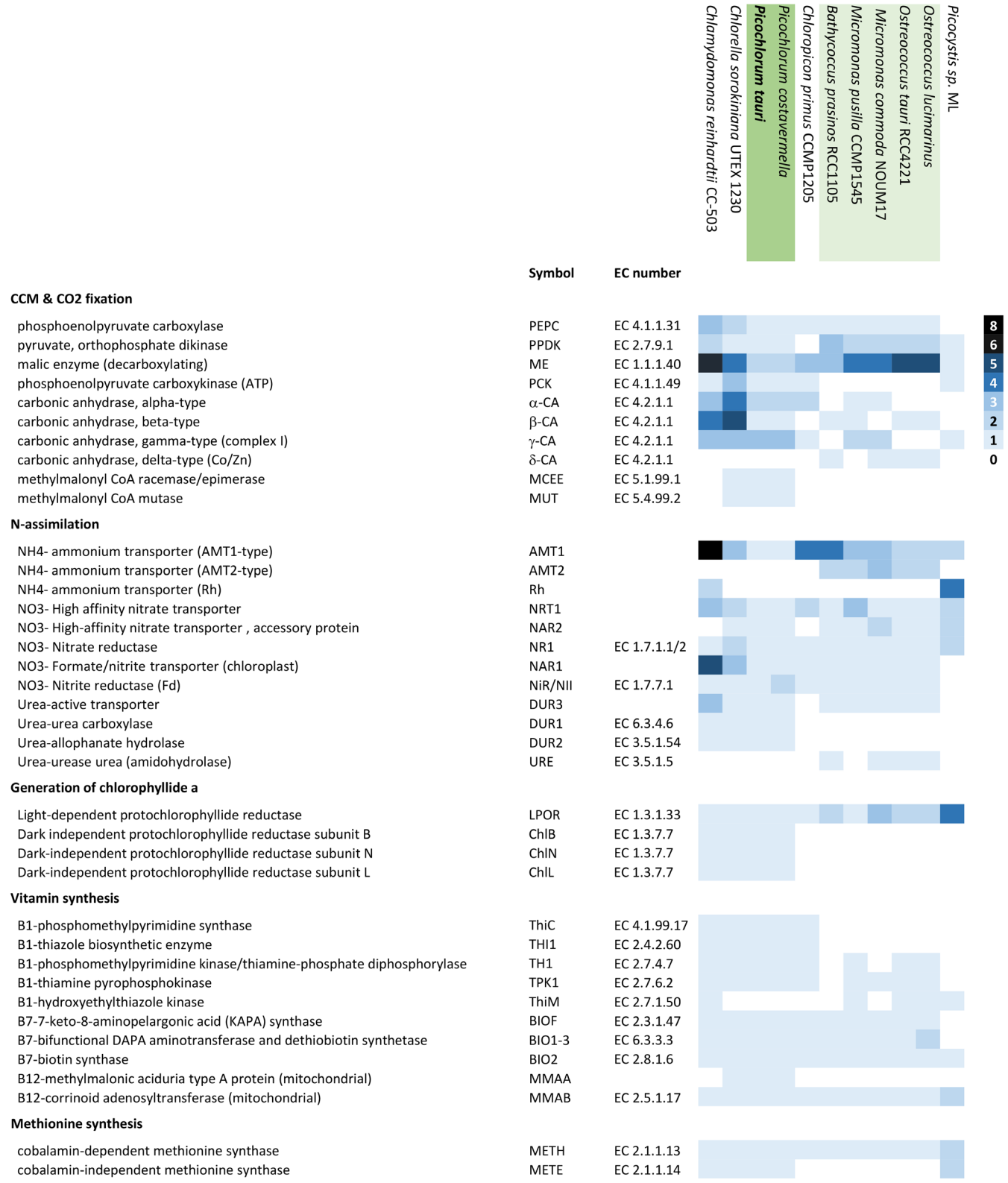

FIGURE 10 | Protein-coding gene content across picophytoeukaryotes. Gene copy number is colour-coded, ranging from white (absence of gene) to navy blue (six copies). Mamiellophyceae are shown in light green. *Picochlorum* spp. are highlighted in green. Accession numbers to predicted proteins are found in Table S12.

carboxylase (DUR1; EC 6.3.4.6) and an allophanate hydrolase (DUR2; EC 3.5.1.54) (Syrett and Leftley 2016). The search showed that all PPEs but *Picocystis* sp. ML have one DUR3 gene, indicating that they are able to take up urea. *P. tauri* is predicted to use the biotin- and ATP-dependent urea degradation DUR1-DUR2 system (Figure 10), while *C. primus* and

the mamiellophyceans (Grimsley et al. 2015) use the nickel-containing urease.

In photosynthetic eukaryotes, chlorophylls are synthesised entirely within the chloroplast from the precursor 5-aminolevulinate to the end product Chl*a* (Beale 2005). The penultimate reaction of Chl*a* biosynthesis consists of the reduction of protochlorophyllide (PChlide) to chlorophyllide (Chlide), which can be catalysed by two biochemically distinct but isofunctional enzymes: (i) L-POR, a light-independent protochlorophyllide oxidoreductase, and (ii) D-POR, an ATP-dependent dark operative enzyme (Armstrong 1998). L-POR is present in all PPEs; however, while *P. tauri* and *C. primus* harbour one *LPOR* gene, the other PPEs have several gene copies (from two to four) (Figure 10). The three plastid-encoded subunits ChlB, ChlL and ChlN of D-POR were only found in the picoalga *P. tauri* (Figure 10, Table S9).

Earlier studies have revealed that many microalgae cannot synthesise diverse combinations of three water-soluble vitamins, that is, vitamin B1 (thiamine diphosphate), vitamin B7 (biotin) and vitamin B12 (cobalamin, Cbl) (Croft et al. 2006; Helliwell 2017). These vitamins are essential for any cell, acting as, or as part of, cofactors for enzymes involved in diverse metabolisms. Each vitamin is synthesised via multiple enzymatic steps. Vitamin B1 is a cofactor for enzymes with critical functions in intracellular carbon and amino acid metabolism. In the genome of *P. tauri* we found all the enzymes required for a thiamine synthesis from pyrimidine and thiazole precursors: a thiamine thiazole synthase (THI4/THI1; EC 2.4.2.60), a phosphomethylpyrimidine synthase (THIC; EC 4.1.99.17), a hydroxymethylpyrimidine/phosphomethylpyrimidine kinase (THIDE; EC 2.7.1.49) and a thiamine pyrophosphokinase (TPK; EC 2.7.6.2) (Figure 10, Table S12). A complete B1 biosynthesis pathway was also found in *C. primus* (Lemieux et al. 2014). As reported previously, algae from the Mamiellophyceae class have an incomplete gene set for B1, and thus depend on exogenous vitamin or its precursors for growth (Paerl et al. 2017) (Figure 10). It was found that the thiazole precursor cHET is a key micronutrient in Mamiellophyceae and that its utilisation is controlled by the activity of the ThiM kinase (EC 2.7.1.50) (Paerl et al. 2017). In *P. tauri*, no ThiM homologue was found. Our survey did not uncover in *Picocystis* sp. ML any of the genes for B1 synthesis. Vitamin B7 is an essential cofactor for many fundamental cellular processes, and serves as a CO_2 carrier in biotin-dependent carboxylation reactions. Genome mining indicated that *P. tauri* has all enzymes for the biotin synthesis from pimeloyl-CoA through the action of 7-keto-8-aminopelargonic acid (KAPA) synthase (BIOF; EC 2.3.1.47), bifunctional dethiobiotin synthetase-diaminopelargonic acid aminotransferase (BIO1-BIO3; EC 2.6.1.62, EC 6.3.3.3) and a biotin synthase (BIO2; EC 2.8.1.6) (Figure 10, Table S12). In that respect, *P. tauri* is comparable to all other PPEs, except *Picocystis* ML, for which genes for BIOF and BIO1-BIO3 were not found (Figure 10). Vitamin B12, a cobalt-containing tetrapyrrole, is one of the most structurally complex cofactors (Warren et al. 2002). It is essential for DNA synthesis, methylation and in some eukaryotes for mitochondrial metabolism. Vitamin B12 synthesis has been well characterised in bacteria, in which a concerted action of at least 20 enzyme-mediated steps is required for a complete B12 synthesis from uroporphyrinogen III (Warren et al. 2002; Modjewski et al. 2024). Rather than mining algal genomes for B12 synthesis pathway reconstruction, it is easier to assess growth in the absence of added B12 vitamin. This is how it was earlier found that *Ostreococcus* spp. are auxotrophs for vitamin B12 (Helliwell 2017; Cooper et al. 2019). We showed here that *P. tauri* does not require exogenous vitamins, including vitamin B12, for growth (Figure 6). It is thus inferred that the alga possessed a complete set of genes for vitamin B12 synthesis. In the genome of *P. tauri*, we also found two genes for the conversion of vitamin B12 into adenosyl-Cbl (AdoCbl), the coenzyme of MUT (Figure 9b): MMAA, which mediates the transport of cobalamin (Cbl) into mitochondria, and MMAB, which generates adenosylcob(III)alamin from cob(I)alamin (Froese et al. 2010). Our survey showed that all other PPEs have an MMAB but lack an MMAA, suggesting that in these species, Cbl is not imported from the cytosol to the mitochondrion. Methylcobalamin (MeCbl), another form of biologically active vitamin B12, is required for methionine synthase METH (EC 2.1.1.13), which interconverts homocysteine and methionine. The survey revealed that all PPEs have one *METH* gene (Figure 10). In nature, there is another type of methionine synthase METE (EC 2.1.1.14), which is cobalamin-independent. It was previously reported that all mamiellophyceans lack a *METE* gene (Helliwell et al. 2011). As revealed here, the *METE* gene is differentially represented among PPEs; it is missing in *C. primus* but present in both *P. tauri* and *Picoscystis* ML (Figure 10).

4 | Discussion

An unprecedented phytoplankton bloom occurred in the Mediterranean Thau lagoon during the winter of 2018–2019 (Lagarde et al. 2021). The important increase in surface Chl*a* took place throughout the month of November and remained at a maximum of 26 μg Chl*a* L^{-1} in the following months of December 2018 and January 2019. The picophytoplankton abundances associated with Chl*a* concentrations were remarkably elevated compared to earlier reports on annual cycles in Thau lagoon (Vaquer et al. 1996; Bec et al. 2005). In this study, we revealed that the winter bloom was primarily due to a green picoalga of the genus *Picochlorum*, which had not been formally identified before in the Thau lagoon. The genus *Picochlorum* together with the genus *Nannochloris* comprises the smallest species within the Trebouxiophyceae class (Henley et al. 2004; Sanders et al. 2022). Trebouxiophyceans are known for their remarkable abilities to withstand harsh conditions and diverse environmental stresses, such as *Chlorella ohadii* isolated from biological sand crust in a desert (Treves et al. 2013) or *Coccomyxa actinabiotis* isolated from a spent fuel cooling pool of a nuclear reactor (Rivasseau et al. 2016). In the literature, species of the genus *Picochlorum* are reported to be halotolerant and thermotolerant (Foflonker et al. 2015, 2018; Krasovec et al. 2018; Weissman et al. 2018; Barten et al. 2022). The intense development of a *Picochlorum* alga in the Mediterranean lagoon in autumn, as well as its sustained presence in the following months in cold waters, revealed a new facet of the resilience of the genus.

The nuclear and organellar genome sequences of the isolated *Picochlorum* species were determined, thus allowing the conduct of whole-genome sequence comparisons with other members of the Trebouxiophyceae class, including the other

Picochlorum species obtained from other geographical sites (USA, Caribbean). As reported here, the ptDNA and mtDNA in *P. tauri* are smaller than their counterparts in other trebouxiophyceans, and yet the gene repertoires are similar irrespective of their lifestyles and niches colonised (Tables S9 and S10). Hence, this suggests that the compactness of the organellar DNAs in *P. tauri* and other *Picochlorum* spp. (Krasovec et al. 2018; Dahlin et al. 2019) is mostly due to a reduced content in non-coding sequences, for example, intronic and intergenic DNA. Lowering the non-coding regions content means reducing the use of N and P (basic elements in the DNA molecules), which are often limited in the marine waters. The nearly unchanged organellar gene sets among trebouxiophyceans thriving in very diverse environments strengthen the recently introduced burst-upon-drift (BUD) model of mitogenome evolution (Butenko et al. 2024). This model proposes that the diversity of mitochondrial genomes is driven by lineage-variable constraints and population genetics. The BUD model is thus in clear contrast with the most prevalent hypotheses, which consider constraints at the level of the gene products, that is, the hydrophobicity hypothesis and the colocation for redox regulation hypothesis.

In comparison to other photosynthetic trebouxiophyceans, species of the genus *Picochlorum* have streamlined genomes (Figure 7) (da Roza et al. 2024; Krishnan et al. 2024), raising the issue of the functions possibly impacted by genome reduction. Through genomic comparison, we evaluated the impact on carbon metabolism. Comparisons showed that the sets of genes for CO_2-concentrating mechanisms in *P. tauri* and other *Picochlorum* spp. were comparable to those in other photosynthetic trebouxiophyceans. The biochemical CCMs identified in *P. tauri* consist of PEPC, a carboxylating enzyme for CO_2 capture, and ME and PCK, which both release CO_2 to the RubisCO active site (Figure 5a). Moreover, three distinct types of carbonic anhydrases for the interconversion of CO_2 and bicarbonate were uncovered in *P. tauri*. In this study, we found that with respect to other trebouxiophyceans, *P. tauri* and other members of the genus *Picochlorum* spp. lack a number of genes encoding enzymes involved in AcCoA-linked pathways: (i) the MS and ICL marker enzymes for the glyoxylate cycle, suggesting that the picoalgae cannot grow heterotrophically on 2C compounds; (ii) ACLY, an ATP- and CoA-dependent citrate lyase, probably hampering the cytosolic production of AcCoA from mitochondrially exported citrate in the *Picochlorum* spp., in stark contrast with most unicellular and multicellular photosynthetic eukaryotes (Fatland et al. 2002); and (iii) PFO and PFL for the anaerobic generation of AcCoA from pyruvate; here, PFO and PFL were found restricted to the *Chlorella* species (Figure 8). In eukaryotes, PFL and PFO are thought to have been acquired via lateral gene transfer in specific lineages (Hug et al. 2010; Stairs et al. 2011). The absence of the *PFL* and *PFO* genes in most surveyed trebouxiophyceans suggests that both anaerobic routes were acquired specifically in one single taxon (*Chlorella*) rather than acquired by the ancestor of the Trebouxiophyceae and lost subsequently in most taxa. The lineage-level comparative study identified two distinct events potentially leading to genome streamlining in the *Picochlorum* genus: a loss of functions (e.g., MS, ICL and ACLY) as well as lower gene copy numbers (ACS, α-CA, PEPC and PCK) (Figure 8).

Propionate, a toxic metabolite, is a natural product of β oxidation of odd-chain fatty acids, and of catabolism of branched-chain amino acids and Methionine. In nature, three different pathways for propionate degradation have been described, which differ by the enzymes involved and the resulting products (Halarnkar and Blomquist 1989; Watson et al. 2016). In *P. tauri*, two distinct pathways were uncovered, namely the most widespread β oxidation-like pathway and the vitamin B12-dependent carboxylation pathway. The presence of the two pathways is expected to confer metabolic flexibility to the picoalga. The β oxidation-like pathway leads to AcCoA, and therefore to a loss of carbon atoms (Figure 9b). The carboxylation pathway leads to the production of succinyl-CoA, which can directly enter the TCA cycle. By circumventing the two decarboxylating steps of the TCA cycle, catalysed by the isocitrate dehydrogenase (EC 1.1.1.41) and the 2-oxoglutarate dehydrogenase (EC 1.2.1.4), the carboxylation pathway allows a net C-fixation and production of substrates for mitochondrial respiration (NADH, succinate) (Figure 9b). In a way, this pathway is reminiscent of the glyoxylate cycle, which also leads to the generation of succinyl-CoA from 2C compounds and was found missing in the picoalga. In the plant *A. thaliana* as well as in the green alga *C. reinhardtii*, the levels of BCAA catabolic enzymes are upregulated in darkness, and during starvation (carbohydrate, nitrogen) (Aubert et al. 1996; Binder 2010; Liang et al. 2019). Assuming that the BCAA degradation occurs in the same conditions in *P. tauri*, a fine balance between the two propionyl-CoA breakdown pathways would allow carbon and energy conservation. In marine waters, dissolved free AAs are an important source of N and C for microbial life (Fuhrman and Ferguson 1986). In marine sediments, anaerobic mineralisation of organic matter results in the production of volatile fatty acids (i.e., acetate, propionate and butyrate), which can be detected in porewaters (Glombitza et al. 2015). If *P. tauri* can take up volatile fatty acids (including propionate) or BCAA (or their precursors) from the environment, these organic molecules could likely serve as sources of C and energy.

The green bloom in the Thau lagoon, initiated in the late autumn (Figure 1b, Table S1), was unprecedented both by its duration (at least 2.5 months) and by the phytoplankton species involved (a pico-trebouxiophycean). To address the preferential development of *P. tauri* over other phytoplankton in the lagoon, several non-exclusive hypotheses could be considered: (i) *Picochlorum* was the predominant PPE in the lagoon in late summer to early autumn (seasonality), (ii) physico-chemical conditions (e.g., temperature, salinity, but also C- and N-sources) were more favourable to trebouxiophyceans than to any other phytoplankton class, and (iii) grazing towards *Picochlorum* spp. was limited. An in-depth ecological description of the Thau lagoon ecosystem in the months preceding the bloom is unfortunately lacking, so none of these hypotheses can be evaluated. In the Thau lagoon, which supports shellfish farming, it is assumed that the PPEs are poorly retained by Pacific oysters, which preferentially feed on phytoplankton larger than 5 μm (Dupuy et al. 2000; Richard et al. 2022). As previously mentioned, the PPEs most common in the Thau lagoon belong to the Mamiellophyceae class, comprising *Ostreococcus*, *Micromonas* and *Bathycoccus* (Courties et al. 1994; Vaquer et al. 1996), with a cell size of 1–2 μm. To assess the metabolic potential of *P. tauri* (not previously described in the lagoon) with that of other small-sized

phytoplankton species, we conducted a large-scale genome comparison. This analysis has shed light on a few functions and traits specific to *P. tauri* that might have contributed to its acclimation in autumn under fluctuating conditions. First of all, we found that *P. tauri* is able to grow in the absence of added vitamins (Figure 6). The other PPEs are auxotrophic for one or two vitamins (Figure 6), and their growth thus depends on the presence of vitamins B1 and B12 (or their precursors) in the environment (Paerl et al. 2015; Helliwell 2017). Even in situations of vitamin B1 or B12 scarcity in the marine waters, *P. tauri* could grow. Since C is the most abundant element in biomass, its low concentration in seawater is rate-limiting and therefore carbon utilisation efficiency is a factor that can influence growth rate and ultimately ecological fitness. The gene survey identified in *P. tauri* an extended set of genes for biochemical and biophysical CCMs, seemingly larger than the gene sets in other PPEs (Figure 8). It is conceivable that the enriched gene repertoire for mechanisms to increase CO_2 near the RubisCO in *Picochlorum*, as compared to the other PPEs (Figure 6), enhances its photosynthetic metabolism. However, we currently have no insights into the photosynthetic efficiency of *P. tauri* at low temperatures (5°C–14°C), which were measured during the winter of 2018–2019 (Table S1). Mucko et al. (2020) reported that the *Picochlorum* strain PMPFPPE4 isolated in the south-eastern Adriatic was able to carry out photosynthesis in the temperature range of 10°C–15°C, with photosynthetic production (μg C μg^{-1} Chl*a* h^{-1}) representing between 20% and 25% of the maximum production measured at 30°C (Mucko et al. 2020). With respect to the autotrophic metabolism, we also found that *P. tauri* has genes for both the light-dependent and light-independent Pchlide oxidoreductases (Figure 10). Therefore, it is expected that *P. tauri* can generate Chl*a* in diverse light conditions, including when suboptimal, for example, in wintertime.

The *Picochlorum* genus is typically described as a group of halotolerant and thermotolerant algae, and several studies highlights its potential in biotechnology (Weissman et al. 2018; Dahlin et al. 2019; Chin-On et al. 2024; Krishnan et al. 2024). Here, we describe *P. tauri*, a new species of the genus, which happened to bloom in late autumn. The high-quality genome sequence determined in this study paves the way to targeted metabolic studies (proteomics and metabolomics). Future work will aim at deciphering the picoalgal adaptive responses to varying environmental conditions as those experienced in the Mediterranean Thau lagoon, in particular N- or P-limitation, and highly fluctuating salinities, temperature and irradiance.

Author Contributions

Béatrice Bec: credit conceptualization, methodology, funding acquisition, resources, formal analysis, data curation, validation, writing – original draft, writing – review and editing. **Franck Lagarde:** credit conceptualization, methodology, project administration, funding acquisition, resources, formal analysis, data curation, validation, writing – original draft, writing – review and editing. **Angélique Gobet:** conceptualization, methodology, funding acquisition, software, resources, formal analysis, visualization, writing – original draft, writing – review and editing. **Riccardo Aiese Cigliano:** methodology, formal analysis, data curation, validation, software, resources, validation, visualization, writing – original draft, writing–review and editing. **Marco Di Marsico:** methodology, software, formal analysis, visualization, writing – review and editing. **Jean-Michel Hermel:** methodology, resources, visualization, writing – review and editing. **Marion Richard:** methodology, resources, formal analysis, validation, writing – review and editing. **Emilie Le Floc'h:** methodology, investigation, formal analysis, writing – review and editing. **Robert van Lis:** data curation, investigation, validation, visualization, writing – original draft, writing – review and editing. **Ariane Atteia:** conceptualization, methodology, project administration, supervision, funding acquisition, investigation, formal analysis, data curation, validation, writing – original draft, writing – review and editing.

Acknowledgements

A.A. and E.L.F. acknowledge support from the Centre National de la Recherche Scientifique (CNRS), B.B. acknowledges support from the University of Montpellier and R.v.L. acknowledges support from the National Research Institute for Agriculture, Food and the Environment (INRAE). A.G., F.L. and M.R. received support from the Institut Français de Recherche pour l'Exploitation de la Mer (IFREMER). This work received financial support from the Ministère de l'Environnement, de l'Agriculture et de l'Alimentation (DPMA), Région Occitanie, Département de l'Hérault, Sète Agglopôle Méditerranée and Department of Oceanography and Ecosystem Dynamic of IFREMER (OVERTE; convention 19/2 217 111), from the Scientific Direction of IFREMER (PICOTHAU; ref. 1000730). This work has also received financial support from the CNRS through the MITI interdisciplinary (pHEATo; 238945), and the support of LabEx CeMEB, an ANR 'Investissements d'avenir' Program (ANR-10-LABX-04-01). Thanks are due to Nicolas Cimiterra, Valérie Derolez, Elodie Foucault, Clarisse Hubert and Gregory Messiaen for their help during the environmental survey (OVERTE project). Thanks are also due to Marie-Line Escande and Joël Rhouy for the help on TEM (Banyuls).

Conflicts of Interest

The authors declare no conflicts of interest.

Data Availability Statement

The ribosomal DNA operon was submitted to GenBank and is available under the accession number ON220582. Data supporting the findings of this work are available within the paper and its Supplementary Information files. Genome sequence datasets generated and analyzed are available at https://data.mendeley.com/datasets/pfd4g6ts72/2 (doi:10.17632/pfd4g6ts72.1). The 18S rDNA sequences used for phylogenetic analysis are available in the same data repository. The complete sequences of the Picochlorum tauri plastid, mitochondrial and nuclear genomes have been deposited in NCBI under BioProject accession number PRJNA1123877. Raw 18S rRNA gene sequences are available in the SRA under BioProject ID PRJNA996377.

References

Almagro Armenteros, J. J., C. K. Sønderby, S. K. Sønderby, H. Nielsen, and O. Winther. 2017. "DeepLoc: Prediction of Protein Subcellular Localization Using Deep Learning." *Bioinformatics* 33: 3387–3395.

Aminot, A., and R. Kérouel. 2004. "Caractéristiques Physicochimiques Majeures." In *Hydrobiologie Des Écosystèmes Marins: Paramètres et Analyses*, 37–41. Edition Ifremer.

Anderson, D. M. 1997. "Turning Back the Harmful Red Tide." *Nature* 388: 513–514.

Andrews, S. 2010. "FastQC: A Quality Control Tool for High Throughput Sequence Data."

Armstrong, G. A. 1998. "Greening in the Dark: Light-Independent Chlorophyll Biosynthesis From Anoxygenic Photosynthetic Bacteria to Gymnosperms." *Journal of Photochemistry and Photobiology B: Biology* 43: 87–100.

Arrigo, K. R., D. H. Robinson, D. L. Worthen, et al. 1999. "Phytoplankton Community Structure and the Drawdown of Nutrients and CO_2 in the Southern Ocean." *Science* 283: 365–367.

Atteia, A., B. Bec, C. Gianaroli, et al. 2024. "Evaluation of Sequential Filtration and Centrifugation to Capture Environmental DNA and Survey Microbial Eukaryotic Communities in Aquatic Environments." *Molecular Ecology Resources* 24: e13887.

Atteia, A., R. van Lis, A. G. Tielens, and W. F. Martin. 2013. "Anaerobic Energy Metabolism in Unicellular Photosynthetic Eukaryotes." *Biochimica et Biophysica Acta* 1827: 210–223.

Aubert, S., C. Alban, R. Bligny, and R. Douce. 1996. "Induction of Beta-Methylcrotonyl-Coenzyme A Carboxylase in Higher Plant Cells During Carbohydrate Starvation: Evidence for a Role of MCCase in Leucine Catabolism." *FEBS Letters* 383: 175–180.

Barten, R., D. J. M. Van Workum, E. de Bakker, et al. 2022. "Genetic Mechanisms Underlying Increased Microalgal Thermotolerance, Maximal Growth Rate, and Yield on Light Following Adaptive Laboratory Evolution." *BMC Biology* 20: 242.

Beale, S. I. 2005. "Green Genes Gleaned." *Trends in Plant Science* 10: 309–312.

Bec, B., Y. Collos, P. Souchu, et al. 2011. "Distribution of Picophytoplankton and Nanophytoplankton Along an Anthropogenic Eutrophication Gradient in French Mediterranean Coastal Lagoons." *Aquatic Microbial Ecology* 63: 29–45.

Bec, B., J. Husseini-Ratrema, Y. Collos, P. Souchu, and A. Vaquer. 2005. "Phytoplankton Seasonal Dynamics in a Mediterranean Coastal Lagoon: Emphasis on the Picoeukaryote Community." *Journal of Plankton Research* 27: 881–894.

Belin, C., D. Soudant, and Z. Amzil. 2021. "Three Decades of Data on Phytoplankton and Phycotoxins on the French Coast: Lessons From REPHY and REPHYTOX." *Harmful Algae* 102: 101733.

Beman, J. M., K. R. Arrigo, and P. A. Matson. 2005. "Agricultural Runoff Fuels Large Phytoplankton Blooms in Vulnerable Areas of the Ocean." *Nature* 434: 211–214.

Binder, S. 2010. "Branched-Chain Amino Acid Metabolism in *Arabidopsis thaliana*." In *The Arabidopsis Book*, vol. 8. American Society of Plant Biologists.

Bolaños, L. M., L. Karp-Boss, C. J. Choi, et al. 2020. "Small Phytoplankton Dominate Western North Atlantic Biomass." *ISME Journal* 14: 1663–1674.

Bolger, A. M., M. Lohse, and B. Usadel. 2014. "Trimmomatic: A Flexible Trimmer for Illumina Sequence Data." *Bioinformatics* 30: 2114–2120.

Braun, H. P., and N. Klusch. 2024. "Promotion of Oxidative Phosphorylation by Complex I-Anchored Carbonic Anhydrases?" *Trends in Plant Science* 29: 64–71.

Brůna, T., A. Lomsadze, and M. Borodovsky. 2020. "GeneMark-EP+: Eukaryotic Gene Prediction With Self-Training in the Space of Genes and Proteins." *NAR Genomics and Bioinformatics* 2: lqaa026.

Brush, M. J., M. Giani, C. Totti, et al. 2020. "Eutrophication, Harmful Algae, Oxygen Depletion, and Acidification." In *Geophysical Monograph Series: Coastal Ecosystems in Transition: A Comparative Analysis of the Northern Adriatic and Chesapeake Bay*, 75–104. John Wiley & Sons.

Buitenhuis, E. T., W. K. Li, D. Vaulot, et al. 2012. "Picophytoplankton Biomass Distribution in the Global Ocean." *Earth System Science Data* 4: 37–46.

Burki, F., A. J. Roger, M. W. Brown, and A. G. Simpson. 2020. "The New Tree of Eukaryotes." *Trends in Ecology & Evolution* 35, no. 1: 43–55.

Butenko, A., J. Lukeš, D. Speijer, and J. G. Wideman. 2024. "Mitochondrial Genomes Revisited: Why Do Different Lineages Retain Different Genes?" *BMC Biology* 22: 15.

Callahan, B. J., P. J. McMurdie, M. J. Rosen, A. W. Han, A. J. A. Johnson, and S. P. Holmes. 2016. "DADA2: High-Resolution Sample Inference From Illumina Amplicon Data." *Nature Methods* 13: 581–583.

Chakraborty, M., J. G. Baldwin-Brown, A. D. Long, and J. J. Emerson. 2016. "Contiguous and Accurate De Novo Assembly of Metazoan Genomes With Modest Long Read Coverage." *Nucleic Acids Research* 44: e147.

Chin-On, R., M. de Boer, C. van de Voort, et al. 2024. "Outdoor Cultivation of *Picochlorum* sp. in a Novel V-Shaped Photobioreactor on the Caribbean Island Bonaire." *Frontiers in Bioengineering and Biotechnology* 12: 1347291.

Chrétiennot-Dinet, M. J., and C. Courties. 1997. "Biodiversity of Unicellular Algae: Example of Pico- and Ultraplanktonic Eucaryotes of the Thau Lagoon." *Vie et Milieu* 47: 317–324.

Chrétiennot-Dinet, M. J., C. Courties, A. Vaquer, et al. 1995. "A New Marine Picoeucaryote: *Ostreococcus tauri* gen. et sp. nov. (Chlorophyta, Prasinophyceae)." *Phycologia* 34: 285–292.

Cooper, M. B., E. Kazamia, K. E. Helliwell, et al. 2019. "Cross-Exchange of B-Vitamins Underpins a Mutualistic Interaction Between *Ostreococcus tauri* and *Dinoroseobacter shibae*." *ISME Journal* 13: 334–345.

Courties, C., A. Vaquer, M. Troussellier, et al. 1994. "Smallest Eukaryotic Organism." *Nature* 370: 255.

Croft, M. T., M. J. Warren, and A. G. Smith. 2006. "Algae Need Their Vitamins." *Eukaryotic Cell* 5: 1175–1183.

Cui, Z., Q. Xu, K. Gibson, S. Liu, and N. Chen. 2021. "Metabarcoding Analysis of Harmful Algal Bloom Species in the Changjiang Estuary, China." *Science of the Total Environment* 782: 146823.

da Roza, P. A., H. Muller, G. J. Sullivan, et al. 2024. "Chromosome-Scale Assembly of the Streamlined Picoeukaryote *Picochlorum* sp. SENEW3 Genome Reveals Rabl-Like Chromatin Structure and Potential for C4 Photosynthesis." *Microbial Genomics* 10: 001223.

Dahlin, L. R., A. T. Gerritsen, C. A. Henard, et al. 2019. "Development of a High-Productivity, Halophilic, Thermotolerant Microalga *Picochlorum renovo*." *Communications Biology* 2: 388.

Delehelle, F., S. Cussat-Blanc, J. M. Alliot, H. Luga, and P. Balaresque. 2018. "ASGART: Fast and Parallel Genome Scale Segmental Duplications Mapping." *Bioinformatics* 34: 2708–2714.

Delmont, T. O., A. M. Eren, J. H. Vineis, and A. F. Post. 2015. "Genome Reconstructions Indicate the Partitioning of Ecological Functions Inside a Phytoplankton Bloom in the Amundsen Sea, Antarctica." *Frontiers in Microbiology* 6: 1090.

Derelle, E., C. Ferraz, M. L. Escande, et al. 2008. "Life-Cycle and Genome of OtV5, a Large DNA Virus of the Pelagic Marine Unicellular Green Alga *Ostreococcus tauri*." *PLoS One* 3: e2250.

Derelle, E., C. Ferraz, S. Rombauts, et al. 2006. "Genome Analysis of the Smallest Free-Living Eukaryote *Ostreococcus tauri* Unveils Many Unique Features." *Proceedings of the National Academy of Sciences of The United States of America* 103: 11647–11652.

Derolez, V., N. Malet, A. Fiandrino, et al. 2020. "Fifty Years of Ecological Changes: Regime Shifts and Drivers in a Coastal Mediterranean Lagoon During Oligotrophication." *Science of the Total Environment* 732: 139292.

Derolez, V., D. Soudant, N. Malet, et al. 2020. "Two Decades of Oligotrophication: Evidence for a Phytoplankton Community Shift in the Coastal Lagoon of Thau (Mediterranean Sea, France)." *Estuarine, Coastal and Shelf Science* 241: 106810.

DiMario, R. J., H. Clayton, A. Mukherjee, M. Ludwig, and J. V. Moroney. 2017. "Plant Carbonic Anhydrases: Structures, Locations, Evolution, and Physiological Roles." *Molecular Plant* 10: 30–46.

DiMario, R. J., M. C. Machingura, G. L. Waldrop, and J. V. Moroney. 2018. "The Many Types of Carbonic Anhydrases in Photosynthetic Organisms." *Plant Science* 268: 11–17.

D'Ortenzio, F., and M. Ribera d'Alcalà. 2008. "On the Trophic Regimes of the Mediterranean Sea: A Satellite Analysis." *Biogeosciences Discussions* 5: 2959–2983.

Dupuy, C., A. Vaquer, T. Lam Hoai, et al. 2000. "Feeding Rate of the Oyster *Crassostrea gigas* in a Natural Planktonic Community of the Mediterranean Thau Lagoon." *Marine Ecology Progress Series* 205: 171–184.

Eckmann, C. A., C. Bachy, F. Wittmers, et al. 2024. "Recurring Seasonality Exposes Dominant Species and Niche Partitioning Strategies of Open Ocean Picoeukaryotic Algae." *Communications Earth & Environment* 5: 266.

Emms, D. M., and S. Kelly. 2019. "OrthoFinder: Phylogenetic Orthology Inference for Comparative Genomics." *Genome Biology* 20: 1–14.

Fatland, B. L., J. Ke, M. D. Anderson, et al. 2002. "Molecular Characterization of a Heteromeric ATP-Citrate Lyase That Generates Cytosolic Acetyl-Coenzyme A in *Arabidopsis*." *Plant Physiology* 130: 740–756.

Fernandez, E., and A. Galvan. 2007. "Inorganic Nitrogen Assimilation in *Chlamydomonas*." *Journal of Experimental Botany* 58: 2279–2287.

Fiandrino, A., V. Ouisse, F. Dumas, et al. 2017. "Spatial Patterns in Coastal Lagoons Related to the Hydrodynamics of Seawater Intrusion." *Marine Pollution Bulletin* 119: 132–144.

Fleury, E., S. Petton, C. Corporeau, A. Benabdelmouna, and S. Pouvreau. 2020. "Observatoire National du Cycle de Vie de l'huître Creuse en France. Rapport annuel ESCOSCOPA 2019." Convention DPMA 2019. RBE/PFOM/PI 2020-1. 71. https://doi.org/10.13155/79902.

Foflonker, F., D. Mollegard, M. Ong, H. S. Yoon, and D. Bhattacharya. 2018. "Genomic Analysis of *Picochlorum* Species Reveals How Microalgae May Adapt to Variable Environments." *Molecular Biology and Evolution* 35: 2702–2711.

Foflonker, F., D. C. Price, H. Qiu, B. Palenik, S. Wang, and D. Bhattacharya. 2015. "Genome of the Halotolerant Green Alga *Picochlorum* sp. Reveals Strategies for Thriving Under Fluctuating Environmental Conditions." *Environmental Microbiology* 17: 412–426.

Froese, D. S., G. Kochan, J. R. Muniz, et al. 2010. "Structures of the Human GTPase MMAA and Vitamin B12-Dependent Methylmalonyl-CoA Mutase and Insight Into Their Complex Formation." *Journal of Biological Chemistry* 285: 38204–38213.

Fuhrman, J. A., and R. L. Ferguson. 1986. "Nanomolar Concentrations and Rapid Turnover of Dissolved Free Amino Acids in Seawater: Agreement Between Chemical and Microbiological Measurements." *Marine Ecology Progress Series* 33: 237–242.

Giordano, M., J. Beardall, and J. A. Raven. 2005. "CO_2 Concentrating Mechanisms in Algae: Mechanisms, Environmental Modulation, and Evolution." *Annual Review of Plant Biology* 56: 99–131.

Glombitza, C., M. Jaussi, H. Røy, M. S. Seidenkrantz, B. A. Lomstein, and B. B. Jørgensen. 2015. "Formate, Acetate, and Propionate as Substrates for Sulfate Reduction in Sub-Arctic Sediments of Southwest Greenland." *Frontiers in Microbiology* 6: 846.

Griffith, M., J. R. Walker, N. C. Spies, B. J. Ainscough, and O. L. Griffith. 2015. "Informatics for RNA Sequencing: A Web Resource for Analysis on the Cloud." *PLoS Computational Biology* 11: e1004393.

Grimsley, N., S. Yau, G. Piganeau, and H. Moreau. 2015. "Typical Features of Genomes in the Mamiellophyceae." In *Marine Protists: Diversity and Dynamics*, 107–127. Springer.

Guan, D., S. A. McCarthy, J. Wood, K. Howe, Y. Wang, and R. Durbin. 2020. "Identifying and Removing Haplotypic Duplication in Primary Genome Assemblies." *Bioinformatics* 36: 2896–2898.

Guillou, L., D. Bachar, S. Audic, et al. 2012. "The Protist Ribosomal Reference Database (PR2): A Catalog of Unicellular Eukaryote Small Sub-Unit rRNA Sequences With Curated Taxonomy." *Nucleic Acids Research* 41: D597–D604.

Gurevich, A., V. Saveliev, N. Vyahhi, and G. Tesler. 2013. "QUAST: Quality Assessment Tool for Genome Assemblies." *Bioinformatics* 29: 1072–1075.

Halarnkar, P. P., and G. J. Blomquist. 1989. "Comparative Aspects of Propionate Metabolism." *Comparative Biochemistry and Physiology Part B: Comparative Biochemistry* 92: 227–231.

Hamlin, F. R. 1988. *Les Noms de Lieux du Département de l'Herault: Nouveau Dictionnaire Topographique et Etymologique*. Imprimerie NotreDame.

Hamon, P. Y., and H. Tournier. 1984. "Evolution de la Biomasse de Mollusques en Élevage Dans l'Etang de Thau de 1980 à 1984." *Revue des Travaux De L'institut des Pêches Maritimes* 48: 33–44.

Helliwell, K. E. 2017. "The Roles of B Vitamins in Phytoplankton Nutrition: New Perspectives and Prospects." *New Phytologist* 216: 62–68.

Helliwell, K. E., G. L. Wheeler, K. C. Leptos, R. E. Goldstein, and A. G. Smith. 2011. "Insights Into the Evolution of Vitamin B12 Auxotrophy From Sequenced Algal Genomes." *Molecular Biology and Evolution* 28: 2921–2933.

Henley, W. J., J. L. Hironaka, L. Guillou, et al. 2004. "Phylogenetic Analysis of the '*Nannochloris*-Like' Algae and Diagnoses of *Picochlorum oklahomensis* gen. et sp. nov.(Trebouxiophyceae, Chlorophyta)." *Phycologia* 43: 641–652.

Hoff, K. J., A. Lomsadze, M. Borodovsky, and M. Stanke. 2019. "Whole-Genome Annotation With BRAKER." In *Gene Prediction: Methods and Protocols*, 65–95. Springer.

Holt, C., and M. Yandell. 2011. "MAKER2: An Annotation Pipeline and Genome-Database Management Tool for Second-Generation Genome Projects." *BMC Bioinformatics* 12: 1–14.

Hood, R. R., E. A. Laws, R. A. Armstrong, et al. 2006. "Pelagic Functional Group Modeling: Progress, Challenges and Prospects." *Deep Sea Research Part II: Topical Studies in Oceanography* 53: 459–512.

Hug, L. A., A. Stechmann, and A. J. Roger. 2010. "Phylogenetic Distributions and Histories of Proteins Involved in Anaerobic Pyruvate Metabolism in Eukaryotes." *Molecular Biology and Evolution* 27: 311–324.

Kanehisa, M., Y. Sato, and M. Kawashima. 2022. "KEGG Mapping Tools for Uncovering Hidden Features in Biological Data." *Protein Science* 31: 47–53.

Kester, D. R., I. W. Duedall, D. N. Connors, and R. M. Pytkowicz. 1967. "Preparation of Artificial Seawater 1." *Limnology and Oceanography* 12: 176–179.

Knight, S., I. Andersson, and C. I. Branden. 1990. "Crystallographic Analysis of Ribulose 1,5-Bisphosphate Carboxylase From Spinach at 2.4 Å Resolution. Subunit Interactions and Active Site." *Journal of Molecular Biology* 215: 113–160.

Kolmogorov, M., J. Yuan, Y. Lin, and P. A. Pevzner. 2019. "Assembly of Long, Error-Prone Reads Using Repeat Graphs." *Nature Biotechnology* 37: 540–546.

Koren, S., B. P. Walenz, K. Berlin, J. R. Miller, N. H. Bergman, and A. M. Phillippy. 2017. "Canu: Scalable and Accurate Long-Read Assembly via Adaptive k-Mer Weighting and Repeat Separation." *Genome Research* 27: 722–736.

Kornberg, H. L., and N. B. Madsen. 1957. "Synthesis of C4-Dicarboxylic Acids From Acetate by a Glyoxylate Bypass of the Tricarboxylic Acid Cycle." *Biochimica et Biophysica Acta* 24: 651–653.

Krasovec, M., E. Vancaester, S. Rombauts, et al. 2018. "Genome Analyses of the Microalga Picochlorum Provide Insights Into the Evolution of Thermotolerance in the Green Lineage." *Genome Biology and Evolution* 10: 2347–2365.

Krishnan, A., L. R. Dahlin, M. T. Guarnieri, J. C. Weissman, and M. C. Posewitz. 2024. "Small Cells With Big Photosynthetic Productivities: Biotechnological Potential of the *Picochlorum* Genus." *Trends in Biotechnology* 43: 759–772.

Kumar, S., G. Stecher, M. Suleski, M. Sanderford, S. Sharma, and K. Tamura. 2024. "Molecular Evolutionary Genetics Analysis Version 12 for Adaptive and Green Computing." *Molecular Biology and Evolution* 41: 1–9.

Lacroux, J., P. Jouannais, A. Atteia, et al. 2022. "Microalgae Screening for Heterotrophic and Mixotrophic Growth on Butyrate." *Algal Research* 67: 102843.

Lagarde, F., A. Atteia, A. Gobet, et al. 2021. "Phénomène d'Eaux Vertes à *Picochlorum* en lagune de Thau Pendant Les Années 2018 et 2019." Observations Environnementales. RST.ODE/UL/LERLR 21-15.

Lagarde, F., V. Le Roy, S. Pouvreau, E. Fleury, and S. Petton. 2025. *ECOSCOPA Network: National Monitoring Network of Mortality and Growth Rates of the Sentinel Oyster Crassostrea gigas*. SEANOE. https://doi.org/10.17882/53007.

Lazzari, P., C. Solidoro, V. Ibello, et al. 2012. "Seasonal and Inter-Annual Variability of Plankton Chlorophyll and Primary Production in the Mediterranean Sea: A Modelling Approach." *Biogeosciences* 9: 217–233.

Legendre, L. 1990. "The Significance of Microalgal Blooms for Fisheries and for the Export of Particulate Organic Carbon in Oceans." *Journal of Plankton Research* 12: 681–699.

Legendre, L., and J. Le Fèvre. 1991. "From Individual Plankton Cells to Pelagic Marine Ecosystems and to Global Biogeochemical Cycles." In *Particle Analysis in Oceanography*, 261–300. Springer Berlin Heidelberg.

Lemieux, C., C. Otis, and M. Turmel. 2014. "Chloroplast Phylogenomic Analysis Resolves Deep-Level Relationships Within the Green Algal Class Trebouxiophyceae." *BMC Evolutionary Biology* 14: 211.

Letunic, I., and P. Bork. 2021. "Interactive Tree of Life (iTOL) v5: An Online Tool for Phylogenetic Tree Display and Annotation." *Nucleic Acids Research* 49: W293–W296.

Liang, Y., F. Kong, I. Torres-Romero, et al. 2019. "Branched-Chain Amino Acid Catabolism Impacts Triacylglycerol Homeostasis in *Chlamydomonas reinhardtii*." *Plant Physiology* 179: 1502–1514.

Luo, W., T. Pröschold, C. Bock, and L. Krienitz. 2010. "Generic Concept in Chlorella-Related Coccoid Green Algae (Chlorophyta, Trebouxiophyceae)." *Plant Biology* 12: 545–553.

Marçais, G., and C. Kingsford. 2011. "A Fast, Lock-Free Approach for Efficient Parallel Counting of Occurrences of k-Mers." *Bioinformatics* 27: 764–770.

McDonald, S. M., J. N. Plant, and A. Z. Worden. 2010. "The Mixed Lineage Nature of Nitrogen Transport and Assimilation in Marine Eukaryotic Phytoplankton: A Case Study of *Micromonas*." *Molecular Biology and Evolution* 27: 2268–2283.

McDonald, T. R., F. S. Dietrich, and F. Lutzoni. 2012. "Multiple Horizontal Gene Transfers of Ammonium Transporters/Ammonia Permeases From Prokaryotes to Eukaryotes: Toward a New Functional and Evolutionary Classification." *Molecular Biology and Evolution* 29: 51–60.

Meyer, M., and H. Griffiths. 2013. "Origins and Diversity of Eukaryotic CO_2-Concentrating Mechanisms: Lessons for the Future." *Journal of Experimental Botany* 64: 769–786.

Mignot, A., R. Ferrari, and K. A. Mork. 2016. "Spring Bloom Onset in the Nordic Seas." *Biogeosciences* 13: 3485–3502.

Modjewski, L. D., V. Karavaeva, N. Mrnjavac, M. Knopp, W. F. Martin, and F. L. Sousa. 2024. "Evidence for Corrin Biosynthesis in the Last Universal Common Ancestor." *FEBS Journal* 292: 827–850.

Mucko, M., J. Padisák, M. Gligora Udovič, et al. 2020. "Characterization of a High Lipid-Producing Thermotolerant Marine Photosynthetic Picoalga From Genus *Picochlorum* (Trebouxiophyceae)." *European Journal of Phycology* 55: 384–399.

Negrete-García, G., J. Y. Luo, C. M. Petrik, M. Manizza, and A. D. Barton. 2024. "Changes in Arctic Ocean Plankton Community Structure and Trophic Dynamics on Seasonal to Interannual Timescales." *Biogeosciences* 21: 4951–4973.

Nei, M., and S. Kumar. 2000. *Molecular Evolution and Phylogenetics*. Oxford University Press.

Paerl, H. W. 2006. "Assessing and Managing Nutrient-Enhanced Eutrophication in Estuarine and Coastal Waters: Interactive Effects of Human and Climatic Perturbations." *Ecological Engineering* 26: 40–54.

Paerl, R. W., E. M. Bertrand, A. E. Allen, B. Palenik, and F. Azam. 2015. "Vitamin B1 Ecophysiology of Marine Picoeukaryotic Algae: Strain-Specific Differences and a New Role for Bacteria in Vitamin Cycling." *Limnology and Oceanography* 60: 215–228.

Paerl, R. W., F. Y. Bouget, J. C. Lozano, et al. 2017. "Use of Plankton-Derived Vitamin B1 Precursors, Especially Thiazole-Related Precursor, by Key Marine Picoeukaryotic Phytoplankton." *ISME Journal* 11: 753–765.

Palmer, T., and P. J. Stansfeld. 2020. "Targeting of Proteins to the Twin-Arginine Translocation Pathway." *Molecular Microbiology* 113: 861–871.

PHYTOBS. 2024. *PHYTOBS Dataset—French National Service of Observation for Phytoplankton in Coastal Waters*. SEANOE. https://doi.org/10.17882/85178.

Pierella Karlusich, J. J., F. M. Ibarbalz, and C. Bowler. 2020. "Phytoplankton in the Tara Ocean." *Annual Review of Marine Science* 12: 233–265.

Piredda, R., M. P. Tomasino, A. M. D'erchia, et al. 2017. "Diversity and Temporal Patterns of Planktonic Protist Assemblages at a Mediterranean Long Term Ecological Research Site." *FEMS Microbiology Ecology* 93: fiw200.

Pryszcz, L. P., and T. Gabaldón. 2016. "Redundans: An Assembly Pipeline for Highly Heterozygous Genomes." *Nucleic Acids Research* 44: e113.

Quinlan, A. R., and I. M. Hall. 2010. "BEDTools: A Flexible Suite of Utilities for Comparing Genomic Features." *Bioinformatics* 26: 841–842.

R Core Team. 2021. *R: A Language and Environment for Statistical Computing*. R Foundation for Statisitical Computing.

Reinfelder, J. R. 2011. "Carbon Concentrating Mechanisms in Eukaryotic Marine Phytoplankton." *Annual Review of Marine Science* 3: 291–315.

Richard, M., B. Bec, L. Bergeon, M. Hébert, C. Mablouké, and F. Lagarde. 2022. "Are Mussels and Oysters Capable of Reducing the Abundances of *Picochlorum* sp., Responsible for a Massive Green Algae Bloom in Thau Lagoon, France?" *Journal of Experimental Marine Biology and Ecology* 556: 151797.

Rivasseau, C., E. Farhi, E. Compagnon, et al. 2016. "*Coccomyxa actinabiotis* sp. nov. (Trebouxiophyceae, Chlorophyta), a New Green Microalga Living in the Spent Fuel Cooling Pool of a Nuclear Reactor." *Journal of Phycology* 52: 689–703.

Saitou, N., and M. Nei. 1987. "The Neighbor-Joining Method: A New Method for Reconstructing Phylogenetic Trees." *Molecular Biology and Evolution* 4: 406–425.

Sanders, C. K., E. R. Hanschen, T. C. Biondi, et al. 2022. "Phylogenetic Analyses and Reclassification of the Oleaginous Marine Species *Nannochloris* sp. "*Desiccata*" (Trebouxiophyceae, Chlorophyta), Formerly *Chlorella desiccata*, Supported by a High-Quality Genome Assembly." *Journal of Phycology* 58: 436–448.

Simão, F. A., R. M. Waterhouse, P. Ioannidis, E. V. Kriventseva, and E. M. Zdobnov. 2015. "BUSCO: Assessing Genome Assembly and Annotation Completeness With Single-Copy Orthologs." *Bioinformatics* 31: 3210–3212.

Smith, D. R., F. Burki, T. Yamada, et al. 2011. "The GC-Rich Mitochondrial and Plastid Genomes of the Green Alga *Coccomyxa* Give Insight Into the Evolution of Organelle DNA Nucleotide Landscape." *PLoS One* 6: e23624.

Stairs, C. W., A. J. Roger, and V. Hampl. 2011. "Eukaryotic Pyruvate Formate Lyase and Its Activating Enzyme were Acquired Laterally from a Firmicute." *Molecular Biology and Evolution* 28: 2087–2099.

Stanke, M., O. Keller, I. Gunduz, A. Hayes, S. Waack, and B. Morgenstern. 2006. "AUGUSTUS: Ab Initio Prediction of Alternative Transcripts." *Nucleic Acids Research* 34: W435–W439.

Stoeck, T., D. Bass, M. Nebel, et al. 2010. "Multiple Marker Parallel Tag Environmental DNA Sequencing Reveals a Highly Complex Eukaryotic Community in Marine Anoxic Water." *Molecular Ecology* 19: 21–31.

Syrett, P., and J. Leftley. 2016. "Nitrate and Urea Assimilation by Algae." In *Perspectives in Experimental Biology*, vol. 2, 221–234. Pergamon Press, Elsevier.

Tabita, F. R. 1999. "Microbial Ribulose 1, 5-Bisphosphate Carboxylase/Oxygenase: A Different Perspective." *Photosynthesis Research* 60: 1–28.

Townsend, D. W., L. M. Cammen, P. M. Holligan, D. E. Campbell, and N. R. Pettigrew. 1994. "Causes and Consequences of Variability in the Timing of Spring Phytoplankton Blooms." *Deep Sea Research Part I: Oceanographic Research Papers* 41: 747–765.

Tragin, M., and D. Vaulot. 2018. "Green Microalgae in Marine Coastal Waters: The Ocean Sampling Day (OSD) Dataset." *Scientific Reports* 8: 14020.

Treves, H., H. Raanan, O. M. Finkel, et al. 2013. "A Newly Isolated *Chlorella* sp. From Desert Sand Crusts Exhibits a Unique Resistance to Excess Light Intensity." *FEMS Microbiology Ecology* 86: 373–380.

Troussellier, M., and J. M. Deslous-Paoli. 2001. "La lagune de Thau: un site atelier pour l'acquisition, l'intégration et la valorisation des connaissances." *Oceanis* 27: 257–289.

Tsuji, Y., A. Mahardika, and Y. Matsuda. 2017. "Evolutionarily Distinct Strategies for the Acquisition of Inorganic Carbon From Seawater in Marine Diatoms." *Journal of Experimental Botany* 68: 3949–3958.

Turmel, M., C. Otis, and C. Lemieux. 2015. "Dynamic Evolution of the Chloroplast Genome in the Green Algal Classes Pedinophyceae and Trebouxiophyceae." *Genome Biology and Evolution* 7: 2062–2082.

Vaquer, A., M. Troussellier, C. Courties, and B. Bibent. 1996. "Standing Stock and Dynamics of Picophytoplankton in the Thau Lagoon (Northwest Mediterranean Coast)." *Limnology and Oceanography* 41: 1821–1828.

Vurture, G. W., F. J. Sedlazeck, M. Nattestad, et al. 2017. "GenomeScope: Fast Reference-Free Genome Profiling From Short Reads." *Bioinformatics* 33: 2202–2204.

Walker, B. J., T. Abeel, T. Shea, et al. 2014. "Pilon: An Integrated Tool for Comprehensive Microbial Variant Detection and Genome Assembly Improvement." *PLoS One* 9: e112963.

Wang, S., W. Lambert, S. Giang, R. Goericke, and B. Palenik. 2014. "Microalgal Assemblages in a Poikilohaline Pond." *Journal of Phycology* 50: 303–309.

Warren, M. J., E. Raux, H. L. Schubert, and J. C. Escalante-Semerena. 2002. "The Biosynthesis of Adenosylcobalamin (Vitamin B12)." *Natural Product Reports* 19: 390–412.

Watson, E., V. Olin-Sandoval, M. J. Hoy, et al. 2016. "Metabolic Network Rewiring of Propionate Flux Compensates Vitamin B12 Deficiency in *C. elegans*." *eLife* 5: e17670.

Weissman, J. C., M. Likhogrud, D. C. Thomas, et al. 2018. "High-Light Selection Produces a Fast-Growing *Picochlorum celeri*." *Algal Research* 36: 17–28.

Williamson, G., A. Bizior, T. Harris, L. Pritchard, P. A. Hoskisson, and A. Javellet. 2024. "Biological Ammonium Transporters From the Amt/Mep/Rh Superfamily: Mechanism, Energetics, and Technical Limitations." *Bioscience Reports* 44: BSR20211209.

Yamori, W., K. Hikosaka, and D. A. Way. 2014. "Temperature Response of Photosynthesis in C3, C4, and CAM Plants: Temperature Acclimation and Temperature Adaptation." *Photosynthesis Research* 119: 101–117.

Supporting Information

Additional supporting information can be found online in the Supporting Information section. **Data S1:** Supporting Information: Figures. **Data S2:** Supporting Information: Tables.